NOTICE

The quality of this microform is heavily dependent upon the quality of the original thesis submitted for microfilming. Every effort has been made to ensure the highest quality of reproduction possible.

If pages are missing, contact the university which granted the degree.

Some pages may have indistinct print especially if the original pages were typed with a poor typewriter ribbon or if the university sent us an inferior photocopy.

Reproduction in full or in part of this microform is governed by the Canadian Copyright Act, R.S.C. 1970, c. C-30, and subsequent amendments.

AVIS

La qualité de cette microforme dépend grandement de la qualité de la thèse soumise au microfilmage. Nous avons tout fait pour assurer une qualité supérieure de reproduction.

S'il manque des pages, veuillez communiquer avec l'université qui a conféré le grade.

La qualité d'impression de certaines pages peut laisser à désirer, surtout si les pages originales ont été dactylographiées à l'aide d'un ruban usé ou si l'université nous a fait parvenir une photocopie de qualité inférieure.

La reproduction, même partielle, de cette microforme est soumise à la Loi canadienne sur le droit d'auteur, SRC 1970, c. C-30, et ses amendements subséquents.

STABILITY OF DEEP-HOLE BTA MACHINING PROCESS

Yemane B. Gessesse

A Thesis

in

The Department

of

Mechanical Engineering

Presented in Partial Fulfillment of the Requirements
for the Degree of Master of Applied Science at
Concordia University
Montreal, Quebec, CANADA

December 1990

ISBN 0-315-64758-2

Canada

ABSTRACT

Stability of Deep-Hole BTA Machining Process

Yemane B. Gessesse

This investigation examines the stability of the BTA (Boring and Trepanning Association) machining process. The BTA-solid tool has been known to give out of roundness or multi-lobes under certain machining conditions. The causes of this phenomenon were not clearly identified and hence effective measures could not be taken to prevent it. In this research work multi-lobe formation or spiralling is identified and measures were taken to prevent its occurrence successfully.

The first step taken in the investigation was determination of lateral natural frequencies of the machine under conditions, similar to those of actual operation. The deep-hole boring machine was connected to a computer through an analog to digital converter and the data obtained was analyzed for frequency distribution. After obtaining the lateral natural frequency distribution of the machine, boring was performed at speeds corresponding to critical values thereby yielding spiralling. The next part of the experiment involved the machining of specimens using a defective tool with its circle-land slightly oversize, at various speeds not within critical range. This also

resulted in the occurrence of spiralling.

The final stage of the investigation was the prevention of multi-lobes formation by modifying the tool. This option was preferred because of the wide variation of lateral natural frequencies with penetration of the tool into the workpiece. Hence modification of the tool was done by placing an additional pad near the circle-land. Operation of the machine at critical speeds proved that spiralling was completely eliminated.

ACKNOWLEDGEMENTS

The author wishes to express his gratitude and appreciation to his thesis supervisor, Dr. V. N. Latinovic for his continuous guidance and support throughout the research.

The financial support of the National Science and Engineering Research Council Grant No. D78 and Fonds Pour La Formation De Chercheurs Et L'Aide A La Recherche Grant No. H56 is acknowledged.

Thanks are also extended to Mr. J. Seeger and the machine shop technicians of Concordia University for thier continued assistance and cooperation.

TABLE OF CONTENTS

PAGE

PAGE

LIST OF FIGURES

LIST OF TABLES

NOMENCLATURE

A	area to be cut [in^2]
A_{di}	deflected area
A_{ni}	nominal area to be cut by cutter i
A_s	shear plane area
A_{sj}	shear plane area for cutter number j
A_{st}	cross-sectional area of the structure
b	width of cut
b_j	width of cut for cutter number j
b_s	slider width
C	constant angle determined experimentally
C_1	arbitrary constant
C_2	arbitrary constant
C_3	arbitrary constant
C_4	arbitrary constant
C	elements of the damping matrix
C_p	unit cutting force [lb]
c_{ci}	side cutting edge length for cutter number i
c_s	specific heat
c_1	damping effect of torsional damper material
c_2	damping due to stuffing box sealant
c_3	damping due to cutter reaction
c_4	structural damping due to workpiece material
c_5	structural damping due to boring bar material
d	depth of cut
D	diameter of tool
E_{st}	Young's Modulus of the structure material

f	frequency
F	cutting force [lb]
F_c	compressive force
F_f	friction force
ΔF_{rl}	force difference
f_n	lateral bending frequency
F_n	normal force
F_r	radial force
F_s	shear force
F_t	tangential force
F_{th}	thrust force
$F(t)$	elements of the force vector
$F_f(t)$	instantaneous feed cutting force
$F_r(t)$	instantaneous radial cutting force
$F_t(t)$	instantaneous tangential cutting force
F_1	cutting force on trailing pad
F_2	cutting force on leading pad
G	slenderness ratio [in/in]
q_p	exponent constant determined experimentally
h	data sampling time
I_{st}	moment of inertia of the area A_{st}
J	mechanical equivalent of heat
K	experimentally determined machining constant
K	elements of the stiffness matrix
K_{ct}	total stiffness at the cutters location
k_s	thermal conductivity
k_1	stiffness due to torsional damper material

k_2	stiffness due to stuffing box sealant
k_3	stiffness due to cutter reaction
k_4	stiffness due to workpiece rigidity
k_5	stiffness due to boring bar-tool assembly rigidity
K_s	cutting force per unit area
l_s	slider length
l_1	length of bar from tool end to stuffing box sealant
l_2	length of bar from sealant to torsional damper
l_3	length of bar from torsional damper to drive unit
l_4	length of workpiece drilled
l_5	unmachined length of workpiece
L_{st}	length of the structure
M	elements of the mass matrix
n	number of cutters
N	number of relevant data collected
n_1	number of lobes formed
P_s	load on slider
$P(f_k)$	power spectral density
Q	total heat flux
q_1	modal coordinate system
Q_1	virtual work of non conservative forces
r_c	chip compression factor
r_j	moment arm for tangential force at cutter number j
R_f	resultant cutting force
$R_{fj}(t)$	instantaneous resultant cutting force
R_1	resultant force in trailing pad direction
R_2	resultant force in leading pad direction

S	shear strength
S_d	stability degree
S_o	shear strength at zero compressive stress
t	time
T	kinetic energy
t_u	uncut chip thickness
T_{av}	average temperature of slider
t_c	cut chip thickness
T_b	total boring torque
T_c	cutting torque
$T_c(t)$	instantaneous torque
V	potential energy
v_s	sliding speed
x	elements of the displacement vector
$\dot{x}$	elements of the velocity vector
$\ddot{x}$	elements of the acceleration vector
X_k	fourier transform normalized with sampling time
$X(f)$	fourier transform of discrete data
$x(nh)$	discrete data sampled at an interval h
z_p	exponent constant determined experimentally
α	rake angle
α_m	mass matrix coefficient in proportional damping
β_k	stiffness matrix coefficient in proportional damping
δ	elemental deflection
ϕ	shear angle
ϕ_p	phase shift angle in machining
η	angle between resultant force and leading pad

η_r	relative velocity
ψ	complimentary angle between the pads
ψ_i	shape function i
κ	approach angle
κ_i	approach angle corresponding to cutter number i
μ_s	mean coefficient of friction
μ_1	coefficient of friction on first pad
μ_2	coefficient of friction on second pad
π	value of pi (3.14)
ρ	mass density of the structure material
ρ_s	density of slider material
σ_n	average compressive normal stress
τ	friction angle
θ_1	angle of first pad from cutting edge
θ_2	angle of second pad from cutting edge
φ	angle between the two pads minus 90°

CHAPTER 1

INTRODUCTION

1.1 Drilling Operations

A number of mechanical components presently manufactured in industry must undergo one type of drilling operation or another for being successfully completed. The type of operation selected usually depends upon these hole requirements:

a) The diameter of the hole

b) The depth of the hole

c) The quality of the hole surface

d) The tolerance of size and roundness error, etc.

These are a few of the deciding factors on the type of drilling process chosen. Even though there are many types of drilling operations available only some important ones are described in this chapter.

Drilling operations involve the removal of metal from highly inaccessible regions. The deeper the hole to be machined the lower the rigidity of the tool, as the rigid tool support is further away from the cutting edge. This phenomenon tends to make the hole making process a complex one, especially for holes of high length to diameter ratio.

Even though most drilling operations originated a few centuries ago, the specialized ones are only a few decades old. Hence, they are far from being perfect in

their performance. Therefore, it is not uncommon to come across some unexplained operational instabilities, while drilling.

In this research work, some aspects of the deep-hole drilling process were investigated thoroughly. Instability of a particular deep-hole boring tool, namely the BTA-solid tool, along with the boring bar assembly was studied in detail. Both dynamic and static stability analysis were done to determine safe operating conditions for the tool.

1.2 Historical Overview

The first hand drills used by man are almost 6000 years old. The cutting edge of the drill was made from a sharp stone and this was attached to a wooden shaft. The shaft was loaded with a heavy piece of stone for developing the required thrust while it was being rotated using a bow handle with a cord attached at its ends. The cord was wrapped around the shaft so that a linear motion to the bow-handle was effectively translated into a rotary motion of the shaft with the cutting stone [1].

The other type of operation which was related to the hole making process, developed around 1700's, was gun boring. It was a finishing operation performed to clean up the rough bore left by the casting process. The method involved mounting a cutting head at the end of a long bar rotated by hand, animal or water power. The longitudinal feed was given to the gun which was fixed to a carriage

hauled along a primitive bed. Due to the inability of producing the required torque and thrust this method was not used for solid gundrilling [2].

The spade drill was the first type of drill used on the boring machine designed and manufactured by Verbruggen, J. and Ziegler, J. in 1758. This machine had the axis of rotation of the gun horizontal. It is believed to be the first of its kind. It was massive in construction and is regarded as the first example of a machine tool for engineering duties. With the growth of technology rising exponentially the drilling operation has come quite far since then.

1.3 Hole Manufacturing Processes

There are a number of drilling and boring operations having diversified types of tools. Most of them use a similar principle; they involve a relative rotary motion between the workpiece and the tool, and require a large thrust for the feed. The working principle of some of the most important drilling operation describing their merits and demerits are given in this chapter. This gives an introduction to the different drilling processes available and provide a general concept in choosing a particular drilling tool over the others.

1.3.1 Spade Drills

The spade drill consists of two cutting edges

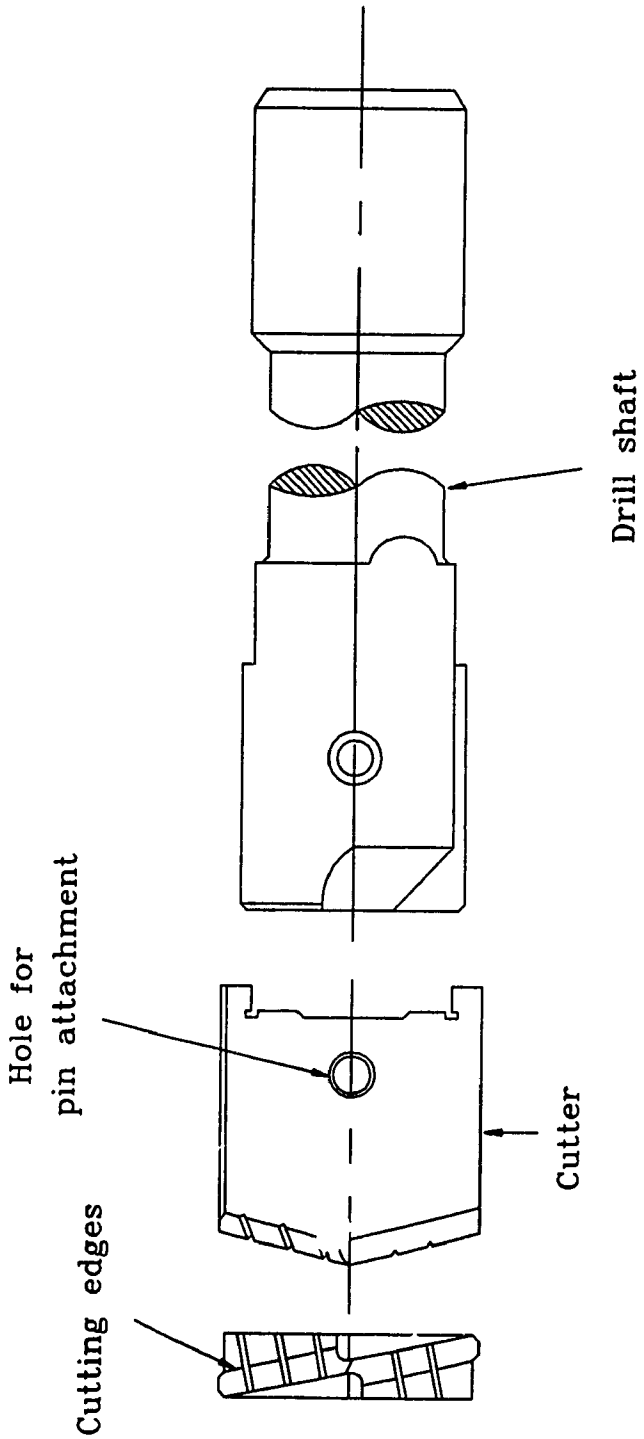

Fig. 1.1 Spade drill

located as shown in Fig. 1.1. Its cutting edges are flat blades slightly inclined from the center towards the periphery, on either side. The symmetry of the two cutting edges helps to balance the radial forces occurring while machining.

The two cutting edges are divided by slots so that metal cut using this cutter forms narrow chips facilitating their removal. Most spade drills have a positive rake angle of five to twelve degrees. The rear end of the cutter has a notch that fits into the holder to simplify the accurate location of the cutting edges, before fastening by a pin.

The main problem associated with this type of drilling tool is the chip removal process. The chips are disposed through the annular gap of the drilled hole and the holder. Another problem associated with this drilling process is excessive heating of the cutting edge due to ineffective cooling by the cutting fluid.

1.3.2 Twist Drills

Twist drills are the most commonly used drilling tools in hole making operations. A twist drill is a highly complex cutting tool used to produce rough holes. There are two cutting edges, on either side, along the diameter and a chisel edge in between. The cutting action usually produces long curling chips which are removed through the twisting flute as shown in Fig. 1.2. Both lips of the drill operate with variable rake angle, inclination angle and clearance

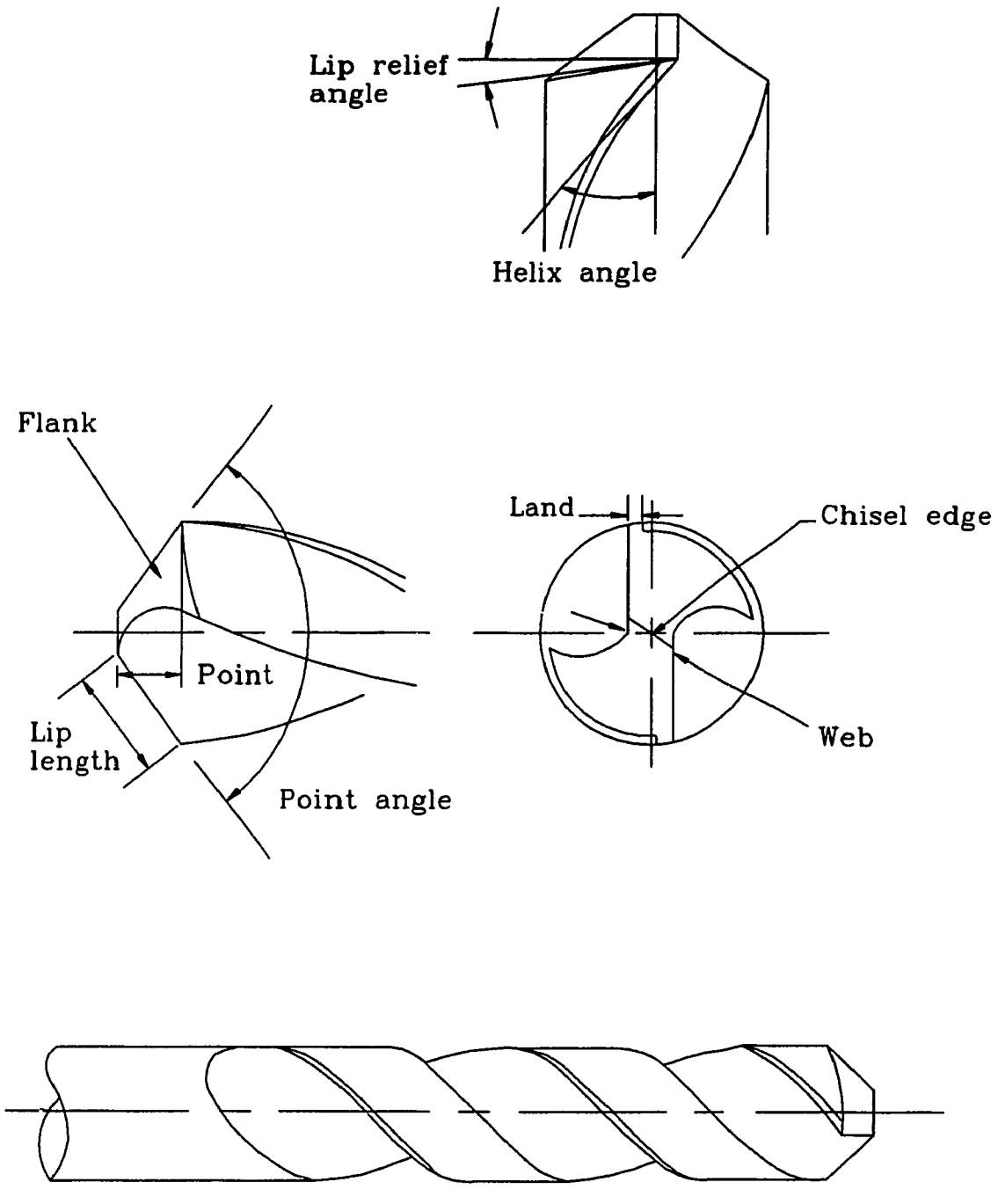

Fig. 1.2 Twist drill

angle along the cutting edges [3].

The torsional strength and difficulty in chip removal make the conventional twist drill inconvenient for deep-hole drilling purposes. However there is a special type of drilling operation using twist drills for deep-hole drilling. It is called " series drilling " and involves drilling a deep hole using more than one drill each designed for the particular range of depth it is going to drill [4].

1.3.3 Boring

The boring operation is one form of drilling that requires a previously machined hole. It is a finishing operation involving the removal of a comparatively small stock of material in order to obtain a smoother surface finish and closer tolerances [5].

Fig. 1.3 shows two of the widely used boring tools. The cutting edge in (a) is supported on a rigid tool post and is fed axially to the rotating work piece. Apparently as can be seen from the figure the length of cut is dictated by the shank length which cannot be too long. Therefore this particular tool is normally used for shallow holes.

The cutting edge shown in (b) on the other hand can be used for relatively deeper holes. The depth is decided by the lateral stiffness of the boring bar. This tool can be used for machining heavy objects with unsymmetrical

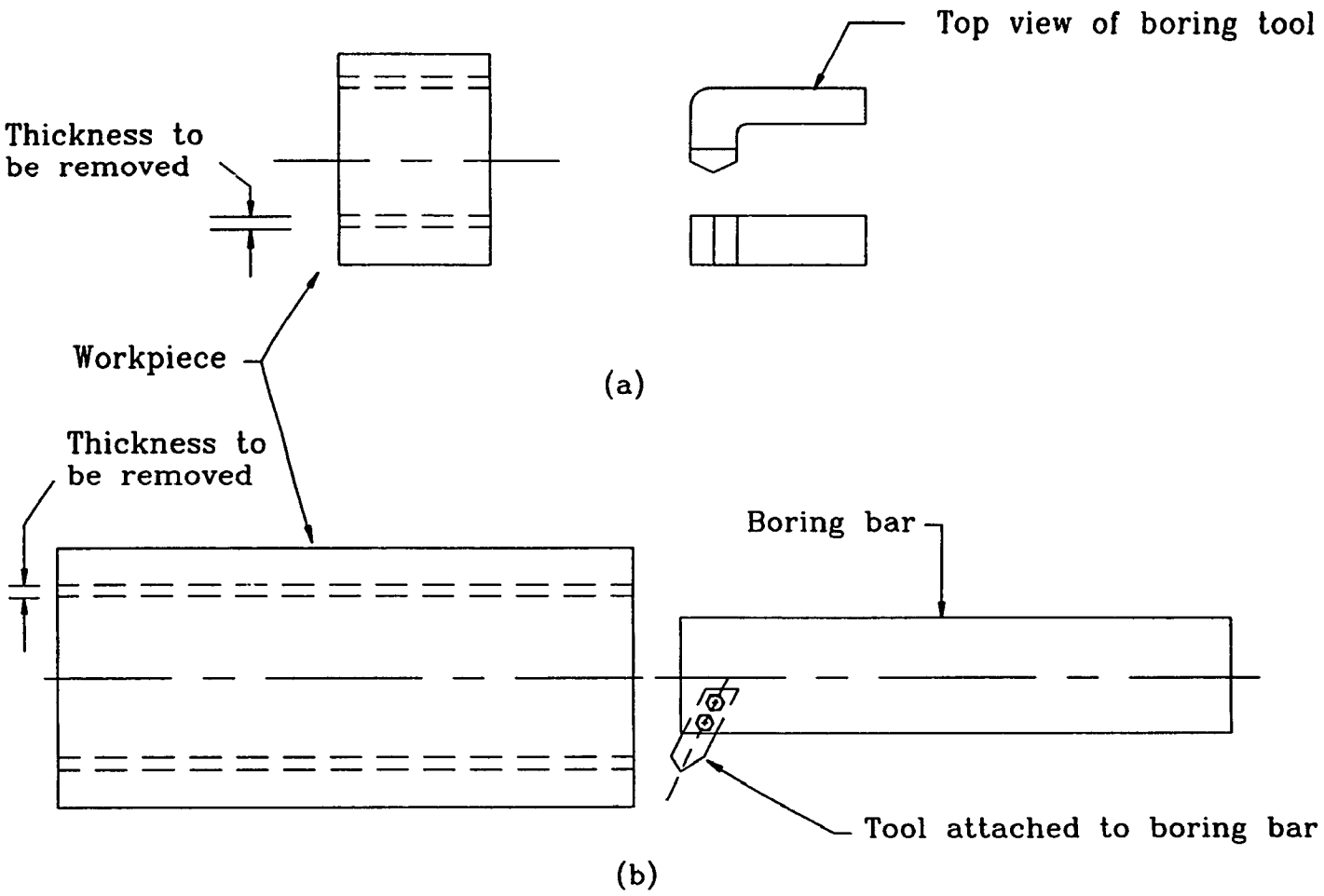

Fig. 1.3 Boring tools used for enlarging existing holes

bodies due to the possibility of giving rotation to the boring bar.

1.3.4 Gundrilling

The gundrill consists of a tube which is brazed to the cutting head as shown in Fig. 1.4. This kidney shaped shank should provide an adequate support to the tool. It should also give the required torsional stiffness to allow a continuous feed [6]. The reason for having the kidney shape for the tube is to provide a passage for the coolant oil flowing to the cutting zone and to provide a return channel on the outside for the return of the swarf and oil mixture.

Gundrill tool has a unique feature which does not exist in the other drills described up to now, it is the inclusion of guide pads. The purpose of these guide pads is multi fold, they help in balancing the remaining unbalanced forces on the cutters, they serve as very good guides for the tool as they are resting on the surface being machined and they yield a very good surface finish by burnishing the surface they are riding on. Because of the supporting action of the pads one can theoretically drill extremely high length to diameter ratio holes ($\approx$ 100).

1.3.5 Ejector Drills

The ejector drill uses a similar principle as the gundrill. It involves the use of cooling fluid to cool

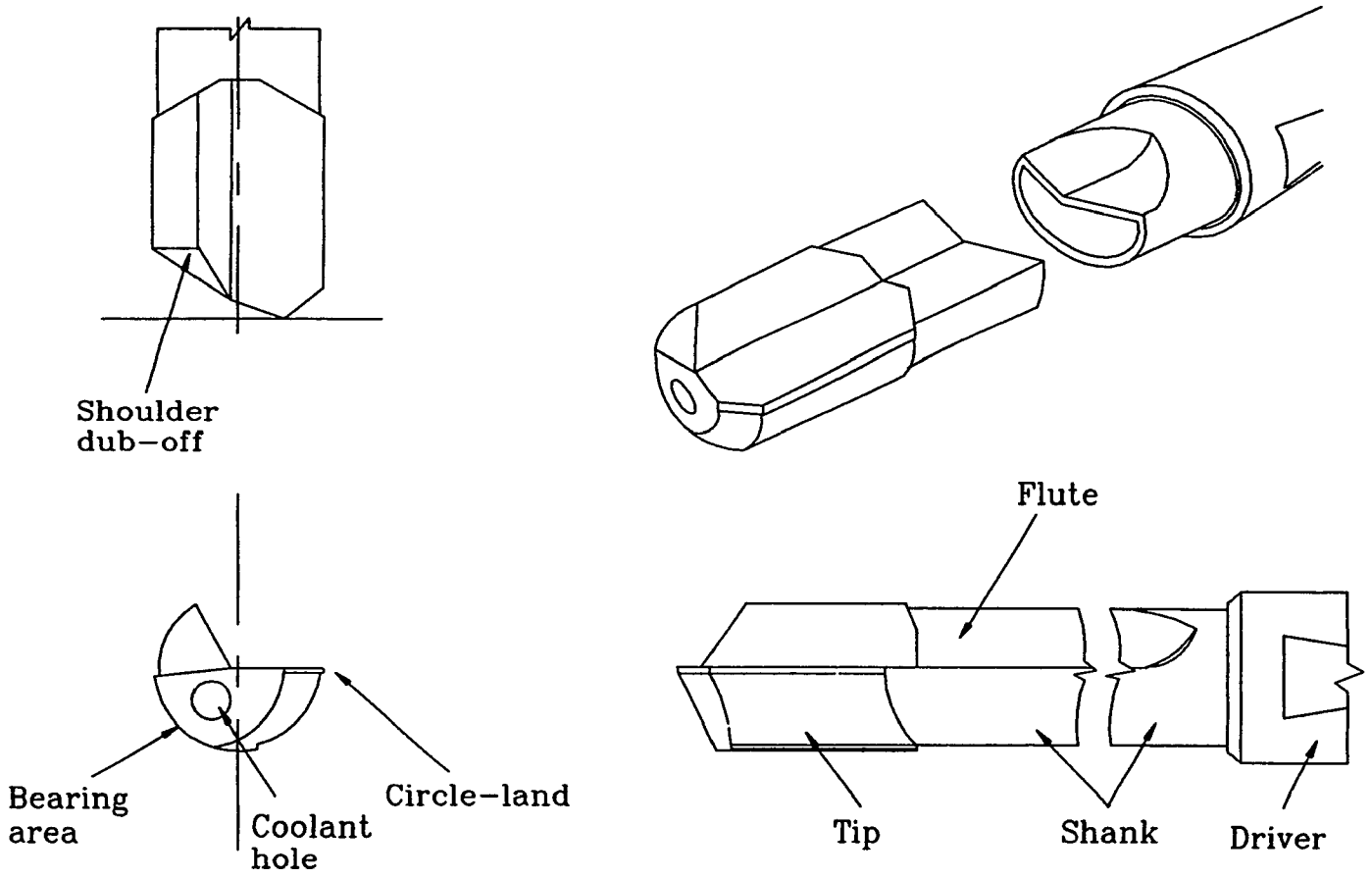

Fig. 1.4 Gundrill

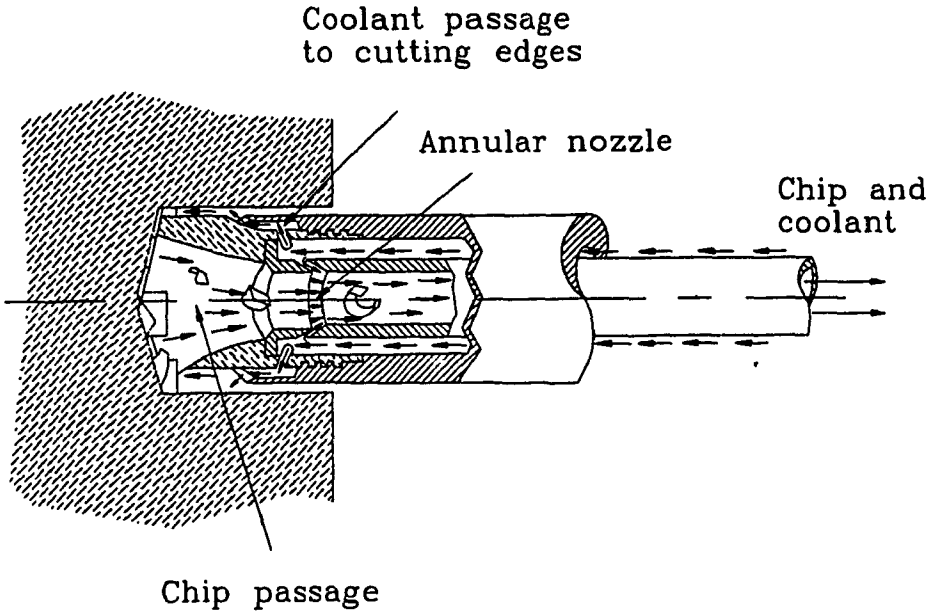

Fig. 1.5 Ejector drill

cutting edges and remove swarf from the cut hole. It is designed to be used on universal machines without the requirement of the special deep-hole drilling apparatus [7,8].

The cutting edges of the ejector drill are distributed over the diameter of the tool. But the effective cutting edge covers a length of one radius even though the total length of the cemented carbide inserts may be more (Fig. 1.5).

The boring bar consists of two steel tubes one inside the other. Oil flows through the annulus towards the cutting edge while part of it returns through the annular-nozzle to the inner tube. The oil circulating around the cutting edge totally depends upon the negative or suction pressure created at the annular-nozzle. The pressure and flow rate of this cooling oil are highly responsible for the effective removal of chips.

1.3.6 BTA-Trepanning Drills

The trepanning drill is unique in its action. Like all the tools using the BTA (Boring and Trepanning Association) [9] principle it requires highly pressurized oil to cool the cutting edge and remove chips. But its peculiarity is that it leaves a solid core while drilling a hole [Fig. 1.6 (a)].

The trepanning tool is mainly used for making holes having internal diameters of 60mm or more. The holes

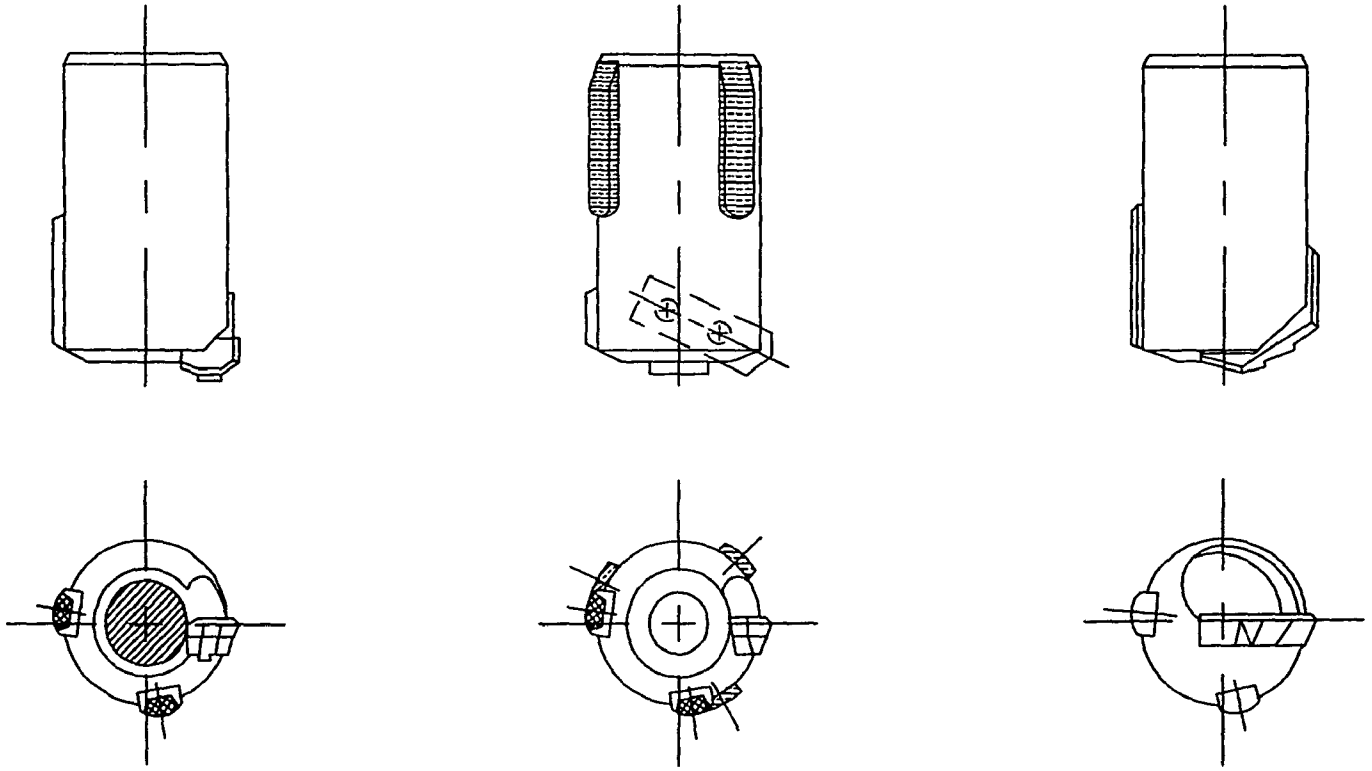

a) Trepanning drill

b) Counter-boring drill

c) Solid boring drill

Fig. 1.6 Typical BTA tools

obtained using this operation are very accurate and straight. The run-out error is minimum if the machine is properly aligned, this being due to the inner core that partially restricts deviations.

A major setback in this operation is the handling of the core especially for very large workpieces weighing in the order of tens of tons. A special and tedious procedure has to be followed in order to avoid plastic deformations coming into picture as a result of the core riding or falling onto the finished surface.

1.3.7 BTA-Counter-Boring Drills

This tool shown in Fig. 1.6 (b) is a tool used in increasing the size of an existing hole. The tool is used in deep hole applications and requires the flow of oil to lubricate and remove the chips. The burnishing pads located as shown in the figure help in giving a smooth surface finish among other functions as stated in BTA tools.

Like the other tools of this type this is also a self-guided tool . One can practically machine holes of up to a hundred of the length to diameter ratio. The accuracy of the resulting hole mainly depends on the premachined hole especially when considering major run-outs. But minor manufacturing surface defects can be corrected after one pass.

1.3.8 BTA-Solid Drills

Fig. 1.6c shows a BTA-solid boring tool. This cutting tool has a cutting edge on one side slightly bigger than one radius. The pointed edge of the tool is slightly offset from the center of rotation avoiding the zero velocity point. There is a small radial cutting force acting on the cutting edge from the center to the apex, balancing a fraction of the cutting force in the radial direction.

The cutting edge is divided into a number of steps in order to ensure the production of narrow chips. This chips are flushed back through the throat of the tool and the center of the boring bar so that the possibility of scratching the burnished surface is avoided.

This drilling technique uses the self-guiding principle. As the tool-boring bar assembly is resting on the workpiece and the cutting and reactive forces are balanced within the workpiece, there is little concern for the weakness of the tool in the lateral direction. Since this research work is using this type of tool, further analysis will involve only the BTA-solid tool.

1.4 Previous Work

The starting point for the analysis of the deep-hole drilling operation is the cutting process. The analytical identification of the cutting forces plays an important role in understanding the process.

Even though metal cutting has been with us for centuries it was only decades ago that Merchant proposed the analytical approach for the determination of forces in the metal cutting operations [10,11]. He identified the two types of cutting known as orthogonal cutting and oblique cutting and gave mathematical model for both. The approach is applicable to most of the metal cutting operations presently used.

The above derivation of forces based on the thin shear plane model assumes a steady state process. In actual machining this is not the case. The cutting force fluctuates, based on many cutting parameters. It can be said to consist of two components, the steady state component and the random component. Rakhit, Sankar and Osman [12] show that the metal cutting forces are predominantly random in nature.

The study made by Arnold [13] showed that the fluctuations in the depth of cut were the main cause of fluctuations in the cutting forces. He studied the stability of the machining process by relating it to self-induced and forced vibrations.

Tobias and Fishwick [14] identified cutting force fluctuations as being due to two types of chatter. They showed that the stability of the system is affected by the workpiece velocity, the workpiece material, shape of the tool and tool shank. They also showed that under certain cutting conditions, the chip thickness variation has a

stabilizing effect.

Merritt [15] developed a theory for the derivation of borderlines of stability for a structure having n-degrees of freedom, assuming no dynamics in the cutting process. He also proposed a stability criterion stating that the directional cutting stiffness must be less than one half the minimum directional dynamic stiffness of the structure for each force orientation to ensure chatter-free performance at all times and speeds. Therefore according to him chatter-free performance can be identified with adequate structural dynamic stiffness for all cutting force orientation.

Long and Lemon [16] in their paper on structural dynamics which is a contribution to machine tool chatter, derived a transfer function for the machine structure and analyzed its dynamic response. The determination of accurate response of the system in the study of stability theory was given by Merritt.

The experimental study made by Kegg [17] finds a representation of the dynamic metal cutting process suitable for use in a linear closed-loop theory of stability of the system composed of machine tool structure and cutting process. This paper which is the third of a four part concurrent presentation on contribution to machine tool chatter is followed by Lemon's and Ackerman's [18] report on applications of self-excited machine tool chatter. They present the utilization of the closed-loop

chatter theory to several actual machine-tool systems. This loop identified by Merritt consists of transfer functions of the cutting process dynamics and structure dynamics with a primary feedba-' path and a regenerative feedback path. Using this closed-loop chatter theory they showed that chatter prevention can be attained by properly allotting dynamic specifications, design criteria, etc.

William Wu [19] presents a model representing the angular oscillation in dynamic orthogonal cutting. He derived the system governing equations based on the work-hardening slip-line field theory in cutting mechanics by taking into account the changes of stress conditions on both the shear plane and the tool-chip interface.

Drilling operation, like all cutting processes has its problem with chatter. Ema, Marui and Fujii [20,21,22,23] by identifying whirling vibrations of the twist drill showed that it was accompanied with a regenerative effect having a phase lag with respect to each revolution. They also showed that a vibration which is a regenerative chatter having a frequency equal to the bending natural frequency of the drill occurred. They have experimentally determined that the frequency per rotation was found to be odd valued but have failed to give satisfactory explanation.

The deep-hole machining operation has managed to reach the stage it is now because of the contributions made by leading researchers working in the field. But because of

the relatively short period since its introduction, it is still far from being perfect in operational performance.

Sakuma, Taguchi and Kinjo [24] investigated K-type and P-type carbide tool cutters for the BTA solid boring tool and were able to identify performance characteristics of the operation. Sakuma, Taguchi and Katsuki [25,26,27] presenting their results of work done on multi-lobe format of holes attempted to explain the reason for occurrence of odd number of lobes only. Investigations by Ema, Marui and Fujii, Sakuma et al reported the number of lobes formed to be equal to the natural bending frequency of the boring bar tool assembly. They also studied the burnishing action of the guide pads and gave the reason for the formation of odd number of lobes as being the resemblance of BTA solid boring tool to that of a four sided cutting edge tool. Since this explanation was not satisfactory Cronjäger, Stockert and Weber [28] gave an explanation relating the position of the cutting edge and guide pads to the formation of odd number of lobes in the BTA deep-hole drilling operation. But then they went on to say that this phenomenon of spiraling is not at all related to the natural bending frequency of the boring bar-tool assembly but rather solely due to the geometry of the cutting edge and angular position of the wear pads.

Griffith [29,30,31] gave an in depth analysis of the reactions occurring at the pad-workpiece interface. He made his study by using a quick stop mechanism to freeze the

cutting action instantaneously. His analysis done on the microscopic level gives a good explanation on the actions of the pads and cutting edge in the BTA solid deep-hole machining operation. He also gave a good explanation on the quality of the surface finish of the hole based on this approach.

Greuner [32,33,34] provided results of different practical aspects of actual deep-hole drilling operations. He showed that solid boring had the highest quality surface finish where as trepanning stood second. Counter-boring was found to have a wider range of surface quality covering the range of both solid boring and trepanning quality. He also showed that even though spiraling could be eliminated by trial and error there was no one who had explained it analytically so far. Another important feature he gave was the use of pull counter-boring to avoid run-out in these operations. Greuner indicated that the gradual introduction of hydraulic controls to alter the damping effect of the torsional Lanchaster damper, can be used for controlling vibrations generated in the system.

The concept of adaptive control was introduced by Tuffentsamer [35]. He specified particular minima and maxima for torque, feed and cutting fluid pressure. If their values lied outside the specified ranges the operation was automatically stopped using the feedback signals. This provided an effective means of prolonging the tool life.

Latinovic and Osman [36,37] have come up with the design of a totally new type of solid boring and trepanning tool. They introduced the concept of unsymmetrical multi-edge cutting tool for the BTA deep-hole machining. Since this tool has a number of cutting edges it was easier to achieve high metal removal rate without compromising the quality of holes and tool life. The superiority of this tool was because of the predetermined cutting force resultant being the starting point for the design of the optimal location of cutters. This ensured that the desired optimum force is exerted on the guide pads resulting in a good surface and longer pad life.

This concept of equal pad forces was further extended for the solid cutter by Torabi and Latinovic [38] and an improvement in hole run-out was seen while the surface finish was slightly inferior to that of the BTA-solid and BTA-multi edge tool with indexable inserts.

Buck [39] and Streicher [40], extending their research in gundrilling operations, showed the similarity between this type of operation and BTA-solid boring. The quality of the surface finish of these two is comparable, except for some instances where gundrills provide slightly better finish. Buck also showed that the type of chip form in gundrill is required to be long and curly to avoid wedging of the chips between the gundrill shank and bored surface. This type of chips are exactly opposite to the broken chips required in BTA drilling to ensure effective

removal.

The stability of deep-hole cutting tools has been studied by Pfleghar [41]. He defined a stability criteria for self-guided tools with two distinct pads based on the reaction force transmitted on them. He identified three types of stability, namely, stable balance, indifferent balance and no balance. These depend on positive, zero and negative reaction force on one of the guide pads respectively. This criterion however does not take into account instabilities that are induced as a result of dynamic cutting force fluctuations on the boring bar tool assembly, leading to regenerative chatter.

The lubricating oil is a very important part of the deep-hole drilling process. Zwingmann [42] and Weber [43] have shown that most of the machining work is converted into heat. It is evident that for the protection of the tool operating at such high temperatures there should be an effective flow of cooling oil. Cooling is not the only function of the oil, it also lubricates rubbing parts and flushes out the chips formed as a result of the cutting process.

1.5 Scope of the Thesis

The main aim of this research work is to identify the dynamic instability of the BTA deep-hole drilling system leading to spiralling while machining. Since the proper analysis of any mechanical system lies in the

identification of its correct mathematical model, a model will be formulated. This proposed model will be studied analytically and experimental frequency response analysis will be carried out to check the mathematical model.

The next stage will be to identify the unstable regions of operations of the deep-hole machining process and generate spiralling based on analytical predictions. Consequently the possible remedies will be suggested and attempted experimentally with intentions of solving the actual problem. Finally, recommendations for future work will be suggested.

CHAPTER 2

ANALYTICAL REPRESENTATION OF CUTTING FORCES IN BTA-SOLID DEEP-HOLE MACHINING

2.1 Geometry of the BTA-Solid Cutter

The deep-hole machining process using BTA-solid tools is similar to conventional hole making operations done using other tools, such as twist drills or spade drills. The basic difference is that, unlike the latter two, the BTA-solid tool does not involve the extrusion action of the chisel edge into the workpiece. Pure cutting can safely be assumed to occur along the length of the cutter. This property enables us to approximately describe the process using the analytical approach.

The geometry of the BTA-solid cutter is the deciding factor for the determination of the cutting forces. As can be seen from Fig. 2.1 the cutter consists of a number of steps which are normally two or three depending upon the size of the tool. The main reason for these steps is to obtain narrower chips, ensuring their effective removal.

The cutter has an apex slightly off from the center avoiding the zero cutting velocity point. The part of the cutter passing over this point usually has a negative rake angle to strengthen it. The steps located on the opposite side of the apex have zero rake angles with the appropriate chip-breaker to guarantee breakage of the chip.

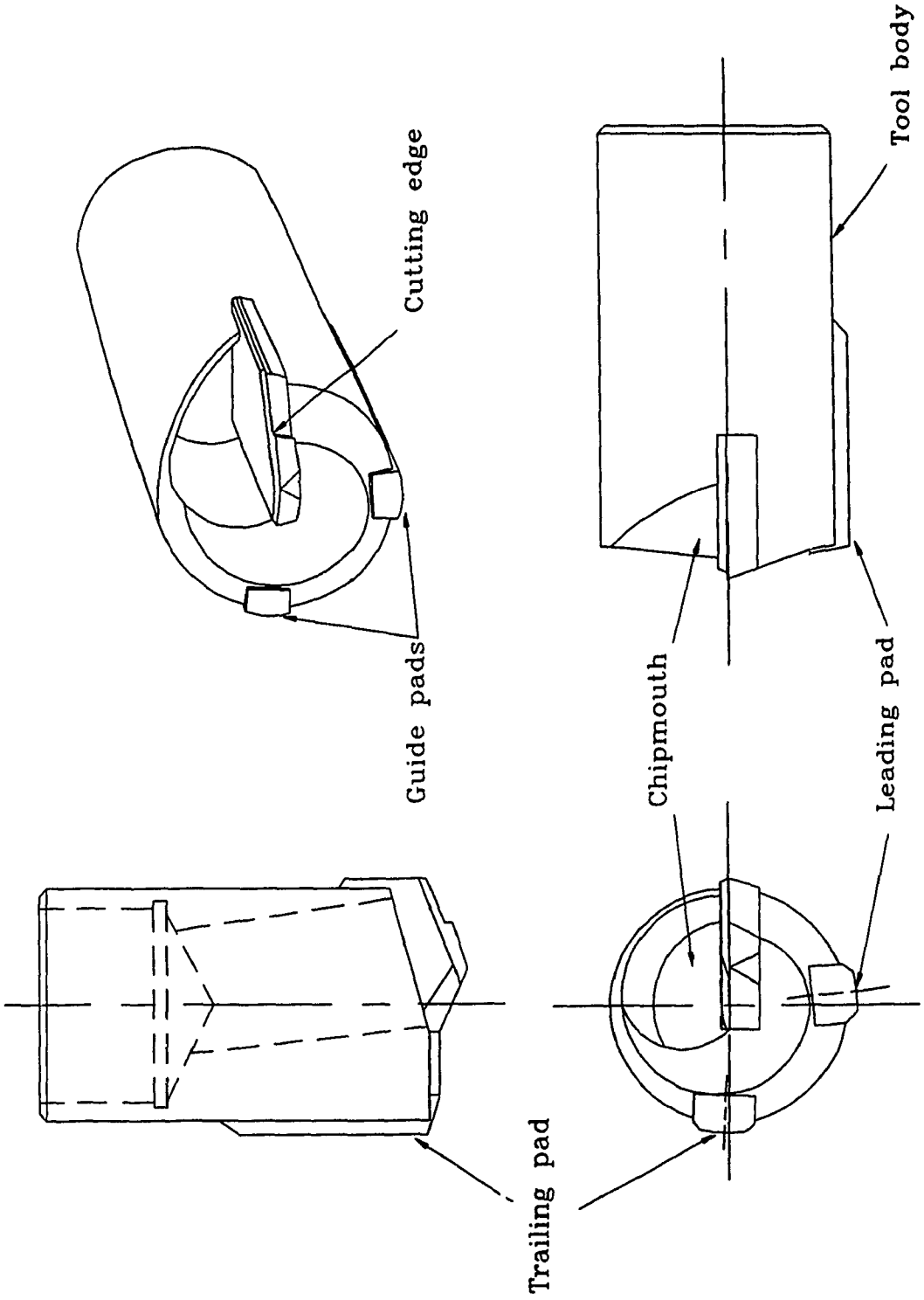

Fig. 2.1 BTA-solid deep-hole boring tool

The resultant of the radial and tangential cutting forces is balanced by the guiding pads while the axial component is transmitted by the boring bar to the drive unit. Despite the fact that there are some assumptions taken to arrive at the mathematical relationship a reasonably accurate cutting force model will be given in the next section.

2.2 Cutting Force Representation of BTA-Solid Tool

The mechanics of the metal cutting process involved in the deep-hole drilling operation is a complex one. The velocity of cut is a linear function of the radius, starting from zero at the center and increasing to a maximum at the outer edge. But, since the direction of the instantaneous velocity vector is perpendicular to the cutting edge, the cutting action can be considered as an orthogonal cutting.

2.2.1 Orthogonal Cutting

Orthogonal cutting is mainly characterized by the direction of the resultant cutting force. Unlike oblique cutting, where the resultant force comprises of three components, the resultant cutting force in orthogonal cutting has only two components in mutually perpendicular directions in space. Fig. 2.2a shows the principle of orthogonal cutting. As seen from the figure the direction of chip flow is in the same direction as the velocity

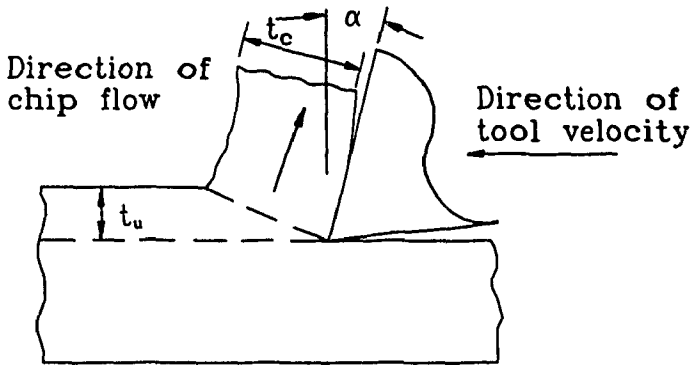

(a)

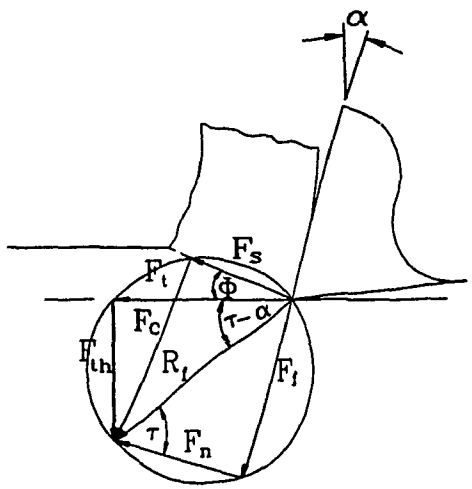

(b)

Fig. 2.2 Orthogonal cutting and cutting force geometry

vector. This is not the case in oblique cutting.

Merchant, in analytically formulating the metal cutting forces for orthogonal and oblique cutting, based his findings on the thin shear plane model [10] which is quite a reasonable approach for high cutting speeds. The shear stress along this shear plane was determined from the Bridgeman relationship relating the shear strength (S_o) at zero compressive stress to that of the actual strength (S) having compressive normal stress (σ_n), under the given cutting conditions.

$$S = \frac{S_o}{\tau - K \tan(\phi + \tau - \alpha)} \qquad (2.1)$$

where

ϕ = shear angle

τ = friction angle

α = rake angle

The value of K is experimentally determined from the following relationship and has an average value of 0.259 for steel [45].

$$K = \frac{S - S_o}{\sigma_n} \qquad (2.2)$$

σ_n is taken to be the average compressive normal stress on the shear plane.

The major assumptions taken by Merchant in arriving at his model are:

(1) The cutting force is a steady one i.e. no fluctuation occurs.

(2) The friction force between the chip and the tool is of dry Coulomb type and is considered as a constant value.

(3) The tool tip is sharp and hence no rubbing, ploughing or extrusion occurs at the relief plane of the tool.

(4) The shear stress and normal stress along the shear plane are uniformly distributed, and

(5) the deformation is two dimensional, implying no side flow.

Based on the above conditions Fig 2.2b can be drawn to show the orthogonal cutting force relationships. The resultant cutting force (R_f) is a sum of the shear force (F_s) and compressive force (F_c). It can also be expressed as the vector sum of the friction force (F_f) and normal force (F_n). Finally the vector sum of the tangential force (F_t) and thrust force (F_{th}) can be drawn to show that it too gives the resultant force (R_f).

From the geometry it can be seen that the tangential and thrust cutting forces are:

$$F_t = R_f \cos(\tau - \alpha) \tag{2.3}$$

$$F_{th} = R_f \sin(\tau - \alpha) \tag{2.4}$$

where

$$R_f = \frac{S\ A_s}{\cos(\tau + \phi - \alpha)} \tag{2.5}$$

$A_s = bd/\sin\phi$ - shear plane area (2.6)

b = width of cut

d = depth of cut

A relationship containing the shear angle, the rake angle and chip compression factor can be obtained from the figure, giving equation (2.7).

$$\tan\phi = \frac{\cos\alpha}{r_c - \sin\alpha} \tag{2.7}$$

$$r_c = \frac{t_c}{t_u} \tag{2.8}$$

where

t_c = cut chip thickness

t_u = uncut chip thickness

The final step in determining the cutting force analytically is finding the right shear angle relationship. A number of researchers working in the field of metal

cutting have proposed many shear angle relationships containing the friction angle and rake angle. Some of the proposed shear angle relationships will be taken up and a derivation of cutting forces for each one performed. This is done and tabulated along Kronenberg's experimental approach for a given, depth and width of cut and workpiece material (Table 2.1).

The next set of equations list the different shear angle relationships given by different researchers.

$$\phi = 45 - \frac{\tau}{2} + \frac{\alpha}{2} \qquad \text{(Merchant)} \qquad (2.9a)$$

$$\phi = 45 - \tau + \frac{\alpha}{2} \qquad \text{(Stabler)} \qquad (2.9b)$$

$$\phi = \frac{1}{2}(C - \tau + \alpha) \qquad \text{(Merchant improved)} \qquad (2.9c)$$

$$\phi = 50 - 0.8(\tau - \alpha) \qquad \text{(Oxley)} \qquad (2.9d)$$

The above relationships shall be used to derive the cutting force required to cut steel that is 0.213in (5.4mm) wide (corresponding to a single step on the BTA-solid cutter) and 0.0047in (0.12mm) deep having a tensile strength of 60000 psi (415 N/mm^2) and shear strength of 31000 psi (214 N/mm^2). Since the necessary angles in finding the cutting force are determined from equation 2.7 and the shear angle relationship, the force can be calculated by using equation 2.3 and 2.4.

The other approach for calculating the cutting force is Kronenberg's empirical formula (2.9e). It uses the extended cutting force law which he experimentally found to be accurate for different width to depth ratios (slenderness ratio), and is given by:

$$F = A\,K_s = \frac{C_p(1000A)^{1-z_p}\,(G/5)^{q_p}}{1000} \qquad (2.9e)$$

where

F = cutting force [lb]

A = area to be cut [in^2]

G = slenderness ratio [in/in]

C_p = unit cutting force [lb]

q_p and z_p are exponents determined from experiments[45]

Table 2.1 Cutting force calculated using different shear angle relationships and Kronenberg's formula.

Force	Merchant	Stabler	Oxley	Merchant imprvd	Kronenberg
R_f(lb)	640	160	255	215	635

As can be seen from the table the cutting force calculated using Merchant's shear angle relationship seems to be in close agreement with Kronenberg's experimental approach. Therefore this one will be used for all subsequent calculations involving cutting force

determination with 0° degree rake angle. However, doing a similar comparison for -30° rake angle shows that Merchant's improved shear angle relationship is in close agreement with Kronenberg's value. Hence, it shall be used for cutting force calculation with the given negative rake angle.

2.2.2 Force on Cutters

This analytical approach of cutting force determination can be directly applied to the BTA-solid drilling tool. Based on the geometry of the tool there are a number of factors affecting the different parameters taken as constant in the derivation. The major discrepancy occurring is as a result of the cutting speed. The speed is varying from zero at the center to a maximum value at the outer edge (Fig. 2.3). For each individual step one can assume an average value based on the midpoint of the step. Even though this could pose a problem in the assumption of the thin shear plane model, it can be seen that the cutting edge is operating at comparatively high speeds.

Force components on the deep hole drilling tool can be derived from the orthogonal cutting conditions which are characterized by the two component forces F_t and F_{th}. The component of the radial force (F_r) and feed force (F_f) are obtained from the thrust force (F_{th}). The tangential force designated by F_t is as shown in Fig. 2.4. For the single step shown the force relationship can be derived as

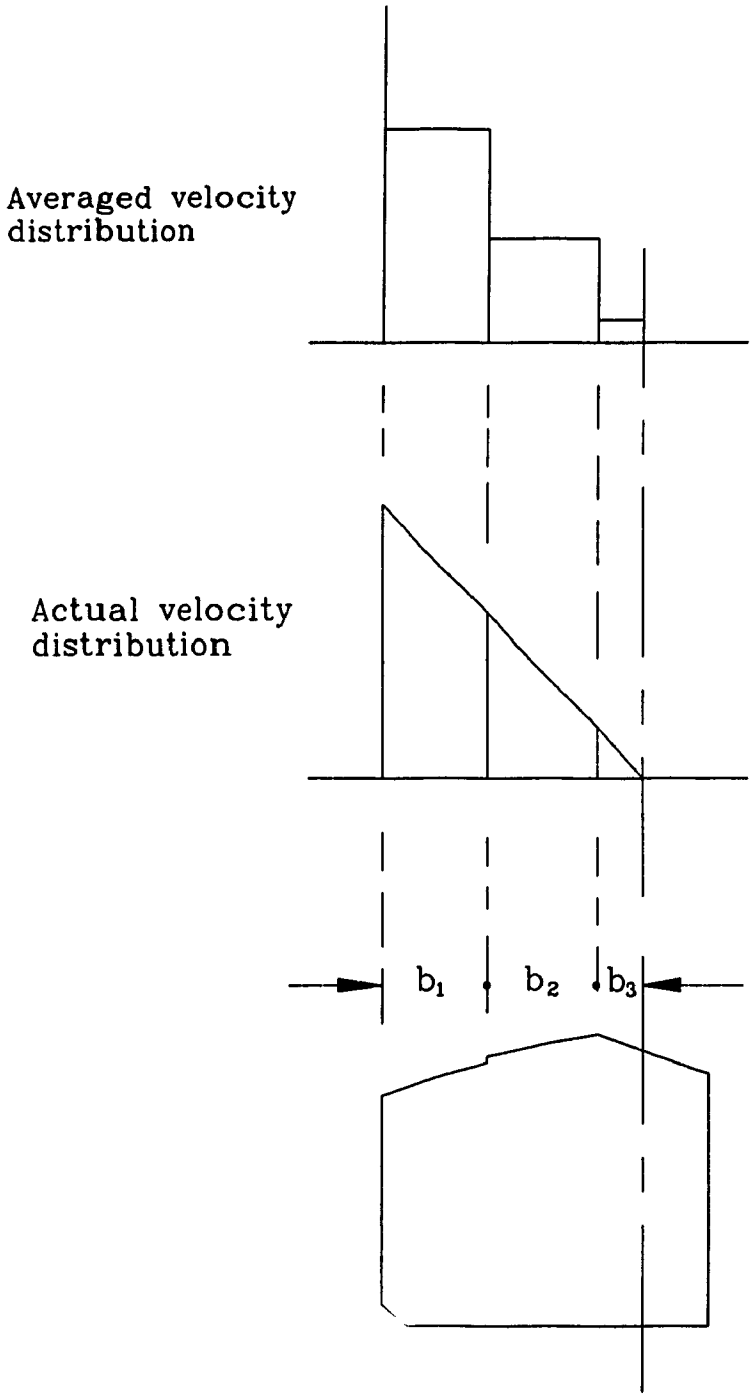

Fig. 2.3 Cutter velocity distribution

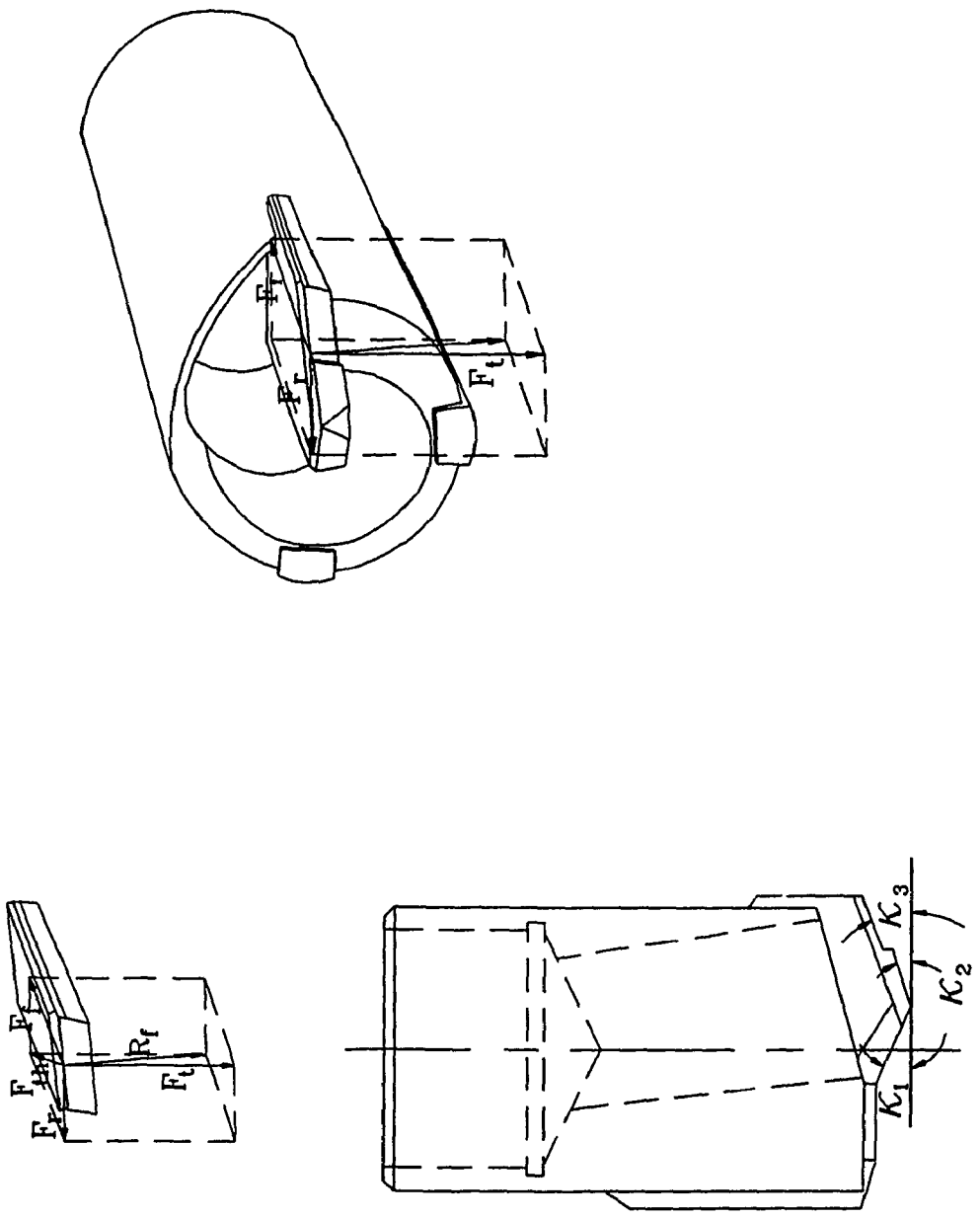

Fig. 2.4 BTA-solid tool cutting force orientation

follows:

$$F_r = F_{th} \sin \kappa \tag{2.10}$$

$$F_f = F_{th} \cos \kappa \tag{2.11}$$

Dividing the cutting edge as shown in Fig. 2.4 into regions, the total force can be obtained by summing up individual forces over the regions. Taking the moment of the tangential force about the center gives the cutting torque (T_c). Considering angles clockwise from the positive x-axis to be negative and the counter-clockwise to be positive the following relationship can be written.

$$F_f = \sum_{j=1}^{n} \frac{S\, A_{sj} \sin(\tau - \alpha) \cos \kappa_j}{\cos(\tau + \phi - \alpha)} \tag{2.12}$$

$$F_r = \sum_{j=1}^{n} \frac{S\, A_{sj} \sin(\tau - \alpha) \sin \kappa_j}{\cos(\tau + \phi - \alpha)} \tag{2.13}$$

$$F_t = \sum_{j=1}^{n} \frac{S\, A_{sj} \cos(\tau - \alpha)}{\cos(\tau + \phi - \alpha)} \tag{2.14}$$

$$T_c = \sum_{j=1}^{n} r_j \frac{S\, A_{sj} \cos(\tau - \alpha)}{\cos(\tau + \phi - \alpha)} \tag{2.15}$$

$$A_{sj} = \frac{b_j\, d}{\cos \kappa_j \sin \phi} \tag{2.16}$$

$$r_j = \frac{b_j}{2} + b_{j-1} + b_{j-2} + \ldots + b_{j-(n-1)} \qquad (2.17)$$

where

n = number of steps

The three mutually perpendicular cutting force components plus the cutting torque were derived for a steady state cutting process. But it has been shown by different researchers that metal cutting process is not steady but rather a random process [12,13,14]. Since the cutting force fluctuation is random in nature one cannot exactly predict the pattern of variation.

Osman, Rakhit and Sankar [12] have shown that the random cutting component is dominant at times and that it might have a magnitude of almost half of the steady state cutting component. Chandrashekar [44] has identified the cutting force in the deep-hole BTA-solid cutter to consist of a steady state component, periodic component and a random component.

The periodic component is obtained as a result of the pattern on the previously cut surface which is the surface to be cut. Once this wavy surface is obtained the consecutive cut is going to follow a similar pattern with a slight phase shift. This results in a regenerative force fluctuation which is periodic in nature. This phenomenon is known as regenerative chatter. Regenerative chatter tends to be a problem if the chatter frequency is at one of the

natural frequencies of the machine.

The mutually perpendicular cutting force components in the BTA-solid drilling can be assumed to be correlated. Fluctuation of one affects the other. These components can be expressed in terms of the resultant cutting force. It can be seen that whatever fluctuation occurs in the resultant force, all the three components are affected proportionally. The following sets of equations are given to show the dependence of the three perpendicular forces and the torque on the resultant cutting force.

$$F_f(t) = \sum_{j=1}^{n} R_{fj}(t) \sin(\tau - \alpha) \cos \kappa_j \qquad (2.18)$$

$$F_r(t) = \sum_{j=1}^{n} R_{fj}(t) \sin(\tau - \alpha) \sin \kappa_j \qquad (2.19)$$

$$F_t(t) = \sum_{j=1}^{n} R_{fj}(t) \cos(\tau - \alpha) \qquad (2.20)$$

$$T_c(t) = \sum_{j=1}^{n} r_j R_{fj}(t) \cos(\tau - \alpha) \qquad (2.21)$$

where

$R_{fj}(t)$ = instantaneous resultant cutting force

$F_f(t)$ = instantaneous feed cutting force

$F_r(t)$ = instantaneous radial cutting force

$F_t(t)$ = instantaneous tangential cutting force

$T_c(t)$ = instantaneous torque

2.2.3 Force on Guiding Pads

In the BTA-solid drilling tool the radial and tangential component of the cutting force are balanced by the pads' reactions. The pads, riding on the previously cut surface, burnish the surface and provide an impeccably smooth finish. This burnishing action occurs as a result of the friction force at the pads. Since this friction force is a product of the normal reactive forces on each pad and the coefficient of friction, it can be seen that these forces vary as the resultant force is altered.

The position of the pads is as shown in Fig. 2.5a. The first pad is located at an angle of θ_1 from the cutting edge and the second one is at an angle of θ_2. Considering the equilibrium of the tool and assuming the coefficient of frictions to be μ_1 and μ_2, the reaction forces at pad one (R_1) and pad two (R_2) are derived.

The resultant of the radial and tangential force can be resolved into two components along the direction of the pads giving F_1, force component in the first pad direction and F_2, force component in the second pad direction. The friction forces coming on the pads are resolved as shown in Fig. 2.5b and added to the force components to give:

$$R_1 = F_1 - \frac{\mu_1 R_1}{\tan \psi} + \frac{\mu_2 R_2}{\sin \psi} \qquad (2.22)$$

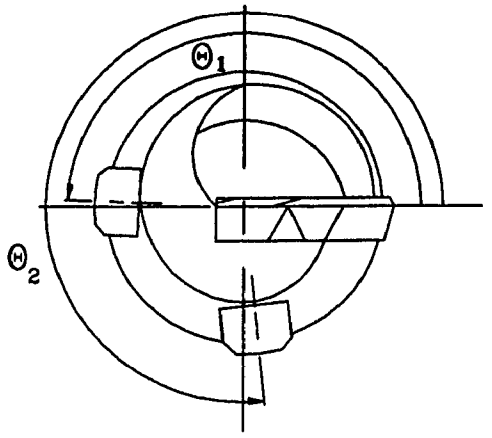

(a)

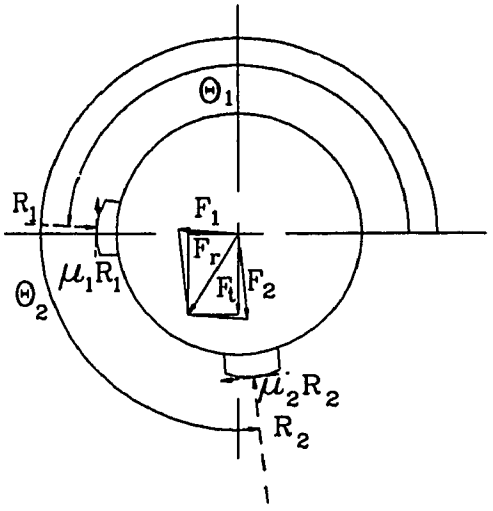

(b)

Fig. 2.5 Pad orientation and cutting force resolution

$$R_2 = F_2 - \frac{\mu_1 R_1}{\sin \psi} + \frac{\mu_2 R_2}{\tan \psi} \qquad (2.23)$$

where

$$\psi = \pi + \theta_1 - \theta_2 \qquad (2.24)$$

From equations 2.22 and 2.23 values of the two normal reaction forces on the pads can be determined.

$$R_1 = \frac{F_1 \sin \psi - F_1 \mu_2 \cos \psi + F_2 \mu_2}{\sin \psi \ (1 + \mu_1 \mu_2) + \cos \psi \ (\mu_1 - \mu_2)} \qquad (2.25)$$

$$R_2 = \frac{F_2 \sin \psi + F_2 \mu_1 \cos \psi - F_1 \mu_1}{\sin \psi \ (1 + \mu_1 \mu_2) + \cos \psi \ (\mu_1 - \mu_2)} \qquad (2.26)$$

where

$$F_1 = \frac{(F_r^2 + F_t^2)^{1/2} \ \sin \eta}{\sin \psi} \qquad (2.27)$$

$$\eta = \theta_2 - 3\pi/2 + \cos^{-1}[F_t/(F_t^2 + F_r^2)^{1/2}] \qquad (2.28)$$

$$F_2 = \frac{(F_r^2 + F_t^2)^{1/2} \ \sin \varphi}{\sin \psi} \qquad (2.29)$$

$$\varphi = \pi - \theta_1 + \cos^{-1}[F_r/(F_t^2 + F_r^2)^{1/2}] \qquad (2.30)$$

Based on the above relationships the variation of

the resultant reaction force direction on the pads with respect to the coefficient of friction on each pad is as shown in Fig. 2.6. The coefficient of friction will be assumed to vary between 0.2 and 0.6 for the three cases, where, first, only the coefficient at the leading pad will vary, second, coefficient at the trailing pad will vary and finally both coefficients will vary.

The mathematical model of the machine taking into account the parts affecting performance of the system will be seen in the next chapter.

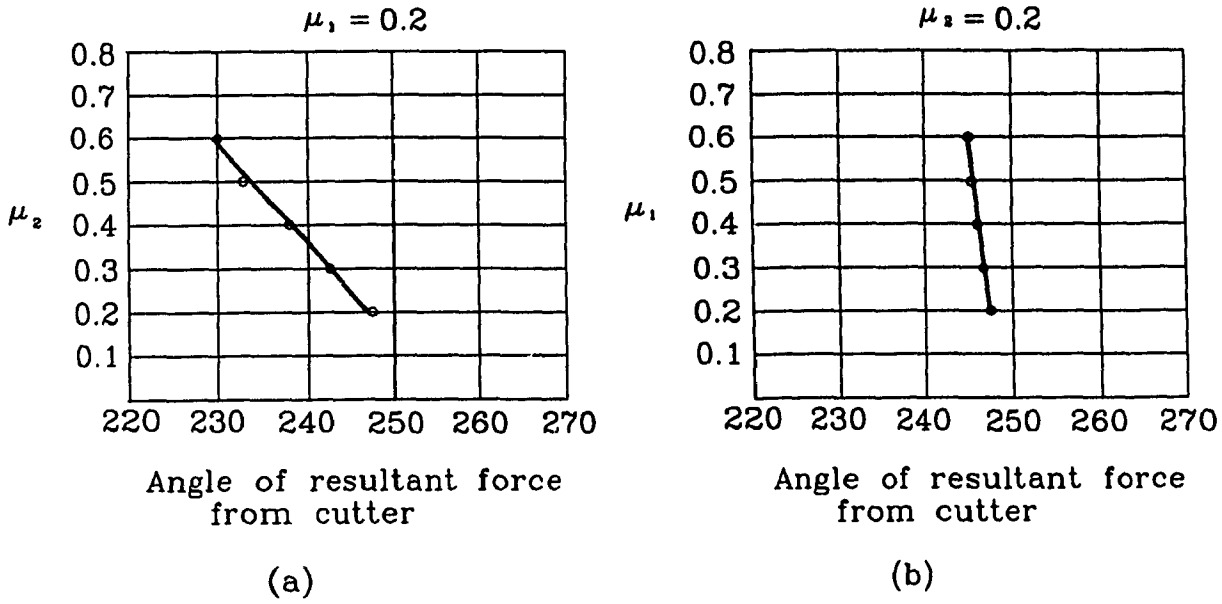

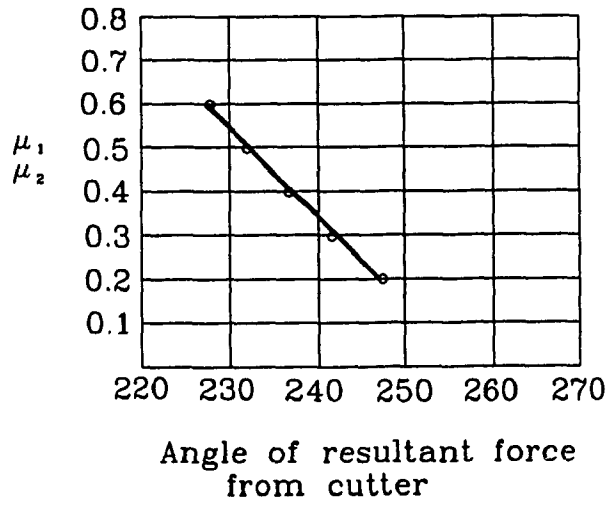

Fig. 2.6 Resultant force angle variation in accordance with coefficient of friction.

CHAPTER 3

MATHEMATICAL MODEL OF THE DEEP-HOLE MACHINE

3.1 The Deep-Hole Machine

An accurate mathematical model is the basis for the analysis of a system. The model of the machine is done step by step taking into consideration the different components and their effects. All important parts affecting the operation shall be seen and their influence studied.

The deep-hole machine consists of a number of components. Each component has its own effect on the performance of the system as a whole. The schematic representation given in Fig. 3.1 shows the different components of the machine and their relative positions.

The principle of operation in the deep-hole machining system involves the introduction of oil to the cutting edges at the pressure head. This pressurized oil passes through the annular gap between the pressure head and the boring bar into the cutting zone. After cooling and lubricating this zone the oil washes out the swarf through the hollow boring bar. Then the oil is properly filtered and recirculated.

The operation of the deep-hole machine depends upon the requirements of the speed, the type of workpiece and the hole specified. In the case of irregularly shaped workpieces the spindle can be held stationary while the

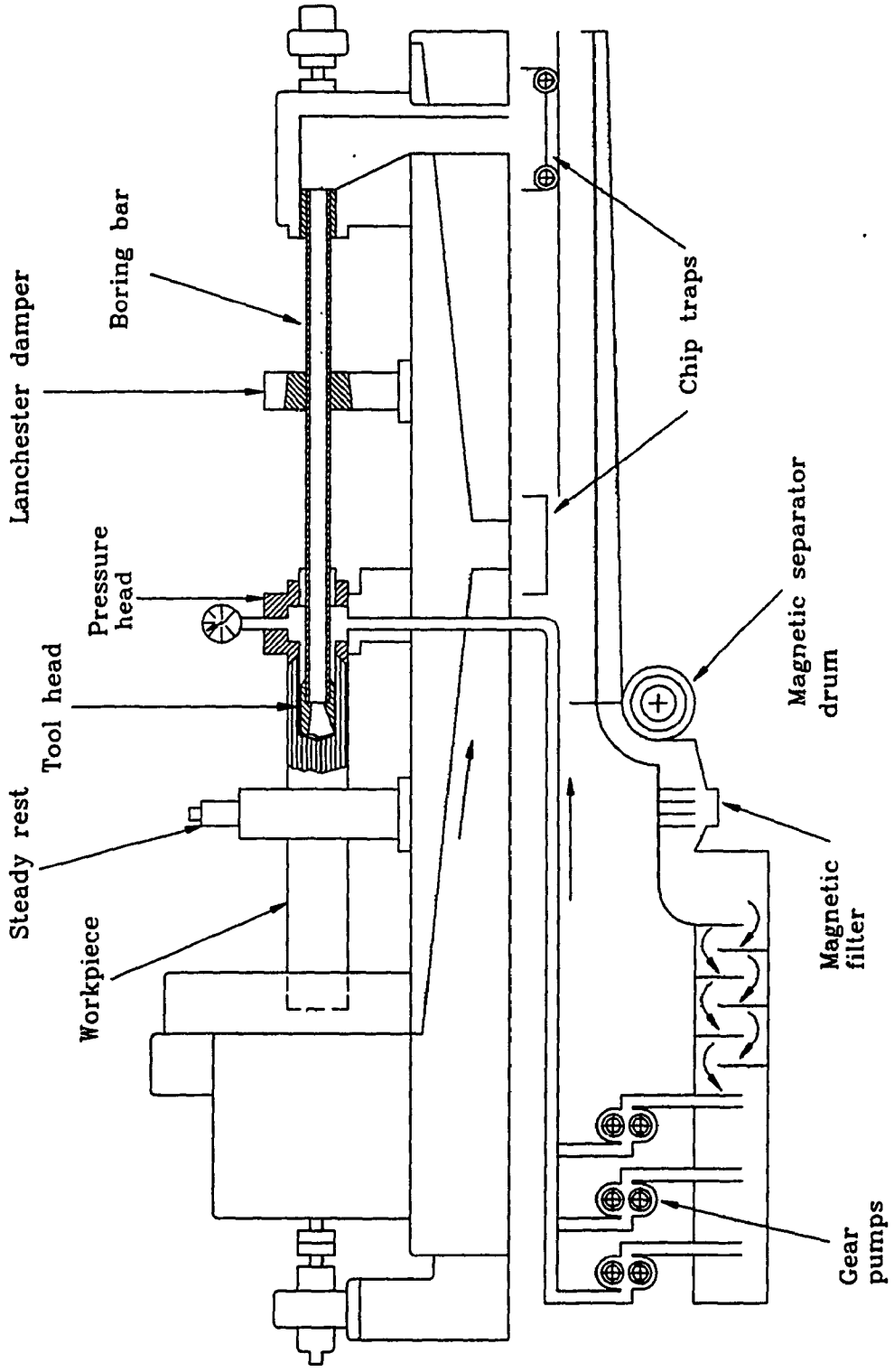

Fig. 3.1 The principle of BTA machining

boring bar is rotated and axially fed. Depending upon the requirements of the operation some drilling is performed while the drive unit is axially fed and the spindle and workpiece are given rotary motion. Final setup arrangement involves the counter-rotation of both the boring bar and spindle, for applications where high cutting speeds are required. This setup gives a hole with minimum run out.

The cutting tool is tightly screwed onto the boring bar giving an almost continuous single piece. Similarly, since there is no relative motion between the chuck and the workpiece, they can be assumed to form a continuous piece.

The boring bar and cutting tool assembly is clamped on to the drive unit. Under normal operating conditions long boring bars are supported by a torsional damper which also helps in increasing the bending stiffness of the bar by supporting it laterally.

The workpiece is clamped by the chuck on one side and supported on the other by a chamfered receding plate in the pressure head. Long workpieces are supported by a steady rest to strengthen them laterally.

All the above mentioned components rest on the massive and highly rigid bed, which in turn is bolted to the ground. Taking into account the relative size of the machine bed and rigid fixtures the model of the deep-hole machine can be reduced to that of the boring bar-cutting tool assembly and spindle-workpiece assembly. The performance of these assemblies will be affected by the

drive unit, torsional damper, steady rest, pressure head and head stock. These components shall be taken up and studied in detail along with their effects on the simplified model.

3.1.1 Drive Unit

The drive unit is the part of the machine that controls the feed motion of the boring bar-tool assembly, and it also has the capability of providing a rotary motion. The feed motion is done by the drive unit sliding on the machine bed. There is a feed power screw right at the center of the bed that is responsible for the axial motion of the drive unit. This implies that the drive unit can be securely attached to the machine bed with close tolerances.

The boring bar-tool assembly is clamped onto the drive unit spindle. The spindle rests on three bearings lubricated by a continuous oil mist supply. The bearings in turn are tightly fixed on the drive unit housing. This attachment mechanism can be considered as a fixed end support for the boring bar-cutting tool assembly, due to its rigid fixtures.

3.1.2 Torsional Damper

This device has a dual purpose. It helps to reduce torsional vibration by applying damping in the torsional mode and also provides an extra support for the boring bar

in the lateral direction. This damper has a base fitted onto the bed guide ways. The base made from mild steel encases a phenolic material split bushing tightened to the boring bar over a tapered surface and a nut.

The torsional damper is secured tightly to the bed at the middle of the boring bar. The phenolic bushing is fixed to the boring bar by tightening it with a nut which controls the amount of pressure on the contact surface near the periphery. It should be tightened enough such that the phenolic material rotates along with the boring bar, but at the same time it should allow the boring bar to creep circumferencially and travel through the bushing axially.

The second arrangements is the travelling damper type. In this arrangement the torsional damper bushing rotates along with the bar and also travels axially with it on the machine bed. This arrangement is a good one if the damper is tightly secured to the guide ways and the motion is controlled by the feed drive unit or some other positive feed mechanism linking the drive unit directly to the damper.

3.1.3 Oil Pressure Head

The oil is introduced into this unit at extremely high pressure. This component, also called oil transfer unit, receives the oil and guides it into the cutting zone while the opposite side is sealed by a stuffing box possessing low stiffness properties. The pressure head

provides a chamfered receding plate to accurately fit the chamfered end of the workpiece for metal to metal seal. The receding plate is fitted to the pressure head on a bearing, and turns with the workpiece. The pressure head is tightly guided on the guide ways and travels along them. The motion of the pressure head is done using the lead screw located on the front side of the machine bed. It can be done manually, or automatically to ensure a clamping force on the workpiece produced hydraulically by the pressure head. Once machining commences the pressure head is locked at its position ensuring that no leakage occurs at the workpiece-pressure head interface.

There is a starting bushing in the pressure head with standard dimensions equal to the diameter of the bore to be machined. This helps in supporting the cutting tool initially on the bushing before it has penetrated into the workpiece fully. The pressure head provides oil under pressure around the periphery of the boring bar-tool assembly. The effect of the pressure head's graphite sealant on the model of the boring bar-tool assembly has to be determined experimentally as will be shown in Chapter 5, however on the spindle-workpiece assembly it can be assumed to provide a simple support.

3.1.4 Headstock

The headstock contains an electric motor driving the spindle with V-belts. These driving and driven shafts carry

a number of gears attached to them providing multi-speeds. The gears are fitted to the shafts by keys. The spindle shaft is hollow and the chuck is attached to it. The chuck clamps the workpiece which in turn rests on the pressure head. The spindle is supported by bearings on either side of the headstock. The headstock is bolted on to the massive machine bed. Lubrication is provided by an internal oil circulating system.

The bearings can be considered as simple supports for the spindle-workpiece assembly.

3.2 Model of the Deep-Hole Machine

In analyzing the deep-hole machine, it is crucial to consider the components affecting the operational performance. The huge machine bed bolted to the ground has a very high stiffness and mass. Therefore, the machine bed can be taken as a rigid body with infinite stiffness, all components resting on it.

It is important to determine the components of prime interest while modelling the machine, they are the once with relatively low stiffness and mass. The components satisfying these criteria are the spindle-workpiece assembly and the boring bar-tool assembly and their respective supports. The interaction between the tool and the workpiece is also an important phenomenon that needs to be accurately modeled.

The modelling of the spindle-workpiece assembly and

boring bar-tool assembly can be done separately. However, the effect of the boring bar-cutting tool assembly on the spindle-workpiece assembly will be taken into consideration and vise versa.

Before proceeding into the model of the spindle-workpiece assembly and boring bar-tool assembly the interaction occurring at the tool-workpiece interface will be seen in detail.

3.2.1 Tool-Workpiece Interface

The interaction occurring at the tool-workpiece interface is a complex one. In order to model the phenomenon occurring accurately a major assumption will be taken, that is since the cutting tool is sharp, there is no rubbing occurring on its flank. Hence the lateral displacement, that could occur on the cutting edge, in a direction opposite to the trailing pad can be considered as a high stiffness, value of which can be calculated from the radial force equation derived in the second chapter.

The radial force fluctuation based on the radial displacement of the cutting edge can be given by equation (3.1) relating the radial displacement to the radial force. Fig. 3.2 gives the cutter geometry and the deflected area variation. As can be seen from the figure, according to the orientation of the cutter, all the deflected areas are added to give the overall equivalent area.

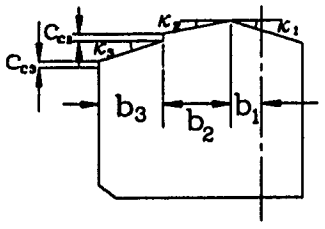

a) Cutter geometry

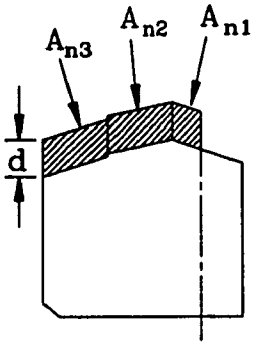

b) Nominal area cut

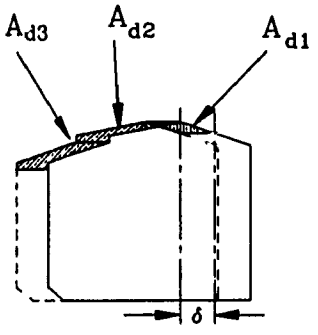

c) Area variation due to small deflection

Fig. 3.2 Cutter interaction with the workpiece for small deflection δ

$$\Delta F_{ri} = \frac{S\, A_{di} \sin(\tau - \alpha)\, \sin \kappa_i}{\sin \phi\, \cos(\phi + \tau - \alpha)} \quad i=1,2,\ldots,n \qquad (3.1)$$

where

$$A_{di} = \delta\, [b_i \tan \kappa_i + c_{ci}] \text{ (deflected area)} \qquad (3.2)$$

ΔF_{ri} = force variation

n = number of steps on the cutter

Based on the above relationship the stiffness value K_{ct} of the cutting edge on the workpiece during the cutting action is given by eqn. 3.3.

$$K_{ct} = \sum_{i=1}^{n} \frac{\Delta F_{ri}}{\delta} \qquad (3.3a)$$

$$= \sum_{i=1}^{n} \frac{S(b_i \tan \kappa_i + c_{ci}) \sin(\tau - \alpha) \sin \kappa_i}{\sin(\phi)\, \cos(\phi + \tau - \alpha)} \qquad (3.3b)$$

where

K_{ct} = total stiffness at the cutters location

δ = deflection at the cutters location

The pad-workpiece interface reaction can be modeled by taking into account the Shaw equation (eqn. 3.4) which studies the temperature rise between two relatively moving objects while a normal force is applied on it. Based on this equation and mechanical property of the involved metals the actual deflection can be calculated by assuming all the deflection occurring on the workpiece to be permanent deformation.

$$T_{av} = 0.707 \frac{Q}{b_s [l_s v_s k_s \rho_s c_s]^{1/2}} \tag{3.4}$$

$$Q = \frac{\mu_s P_s v_s}{J} \tag{3.5}$$

where

T_{av} = average temperature of slider

Q = total heat flux

b_s = slider width

l_s = slider length

v_s = sliding speed

k_s = thermal conductivity

ρ_s = density

c_s = specific heat

μ_s = mean coefficient of friction

P_s = load on slider

J = mechanical equivalent of heat

The deformation associated with the pads is directly proportional to the relative velocity and the load between the two sliders. Even though it could lead to an instability of the system due to fluctuating forces, by unevenly burnishing the cut surface, the stiffness equivalent is too high to make a significant difference in frequency as compared to fixed support.

The force coming on the slider (pads) is too little to bring about a pronounced effect on the overall system due to the comparatively large area of contact.

3.2.2 Spindle-Workpiece Assembly

The spindle-workpiece assembly can be considered as a single shaft with variable cross sectional area supported by simple supports where the spindle is resting on the bearings and the chamfered end of the workpiece is resting on the pressure head. This is mainly because the bearing stiffness is relatively high.

The effect of the boring bar-tool assembly can be considered as a stiffness and a damper at the point where it contacts the spindle-workpiece assembly (Fig. 3.3). Due to the cutting action occurring there is a continuous contact between the tool and the workpiece. Hence the stiffness and the damping properties of the boring bar-tool assembly act continuously on the spindle-workpiece assembly. However its effect on the frequency distribution is quite small and can safely be neglected.

The equation of motion of the spindle-workpiece assembly can be expressed using the standard matrix form as follows;

$$[M]\{\ddot{x}\} + [C]\{\dot{x}\} + [K]\{x\} = \{F(t)\} \qquad (3.6)$$

where

$[M]$ = the mass matrix

$[C]$ = the damping matrix

$[K]$ = the stiffness matrix

$\{\ddot{x}\}$ = the acceleration vector

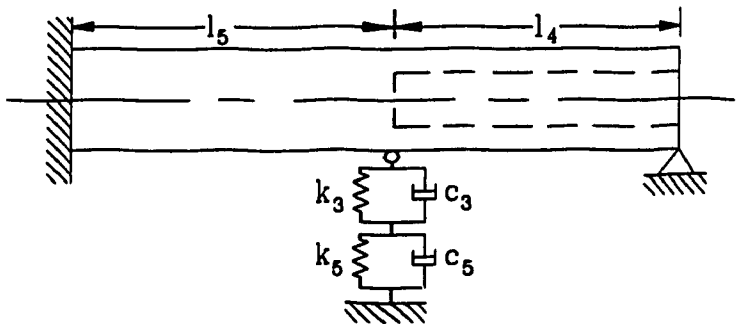

a) Reduced workpiece-spindle model

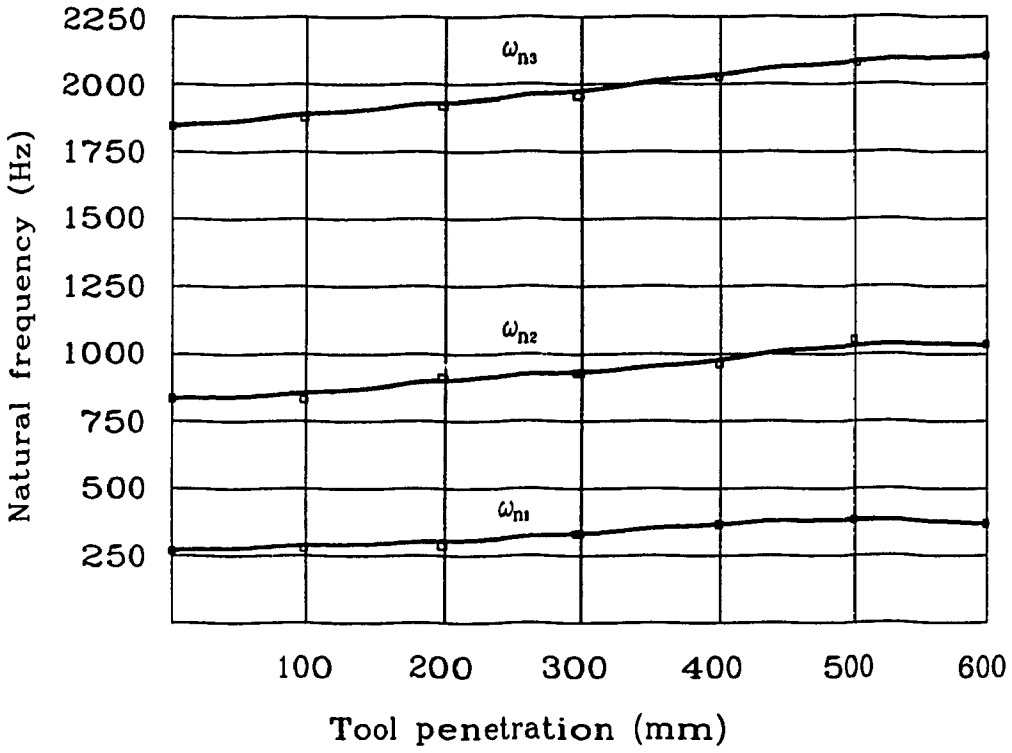

b) Workpiece lateral natural frequency variation

Fig. 3.3 Model of workpiece-spindle assembly

$\{\dot{x}\}$ = the velocity vector

$\{x\}$ = the displacement vector

$\{F(t)\}$ = the force vector

Due to the variation of the cross sectional area of the spindle-workpiece assembly the finite element method is used to discretize the continuous system. The principles involved in discretizing the system and studying it using modal analysis is given in appendix A.

The mass matrix and stiffness matrix for a single element is given by eqns. 3.7 and 3.8 respectively.

$$M = \frac{\rho A_{st} L_{st}}{420}\begin{bmatrix} 156 & 22L_{st} & 54 & -13L_{st} \\ & 4L_{st}^2 & 13L_{st} & -3L_{st}^2 \\ & & 156 & -22L_{st} \\ \text{SYM} & & & 4L_{st}^2 \end{bmatrix} \tag{3.7}$$

$$K = \frac{E_{st} I_{st}}{L_{st}^3}\begin{bmatrix} 12 & 6L_{st} & -12 & 6L_{st} \\ & 4L_{st}^2 & -6L_{st} & 2L_{st}^2 \\ & & 12 & -6L_{st} \\ \text{SYM} & & & 4L_{st}^2 \end{bmatrix} \tag{3.8}$$

where

ρ = mass density of the structure material

A_{st} = cross-sectional area of the structure

L_{st} = length of the structure

I_{st} = moment of inertia of the area A_{st}

E_{st} = Young's modulus of the structure material

The direct stiffness method can be used to assemble adjacent corresponding matrices. The principle underlying this method is work and strain energy being scalar quantities. The strain energy of a structure is the sum of the strain energy contributions of all of its elements.

The damping matrix can be taken as Rayleigh damping. This assumption can be justified if the damping occurring is of structural type (eqn. 3.9).

$$[C] = \alpha_m [M] + \beta_k [K] \qquad (3.9)$$

The damping occurring as a result of the boring bar tool assembly can be reduced to a viscous damper based on the structural damping value of the boring bar. However the total damping of a structural system is only 3 - 4% of the critical damping which can safely be neglected. Therefore equation 3.6 reduces to equation 3.10.

$$[M](\ddot{x}) + [K](x) = (F(t)) \qquad (3.10)$$

In mathematically computing the system's frequency distribution the model was further reduced to the workpiece only, because of the huge relative size difference between the spindle and the workpiece used for the experiment. Hence the end conditions of the workpiece on the spindle side was taken as a fixed end support while on the pressure head side it was taken as simple support. Since the

workpiece was relatively short, the steady rest normally used for laterally supporting long ones was not used. Fig. 3.3b gives a plot of the natural frequency variation with respect to the tool penetration of the workpiece i.e. the first three modes are plotted as the tool bores through the entire workpiece.

3.2.3 Boring Bar-Cutting Tool Assembly

The boring bar-cutting tool assembly is treated as a single unit supported by a fixed support at one end and a flexible support at the cutter end and the graphite sealant position.

The model of the boring bar-cutting tool assembly is done in the same way as the spindle-workpiece was done. Modal analysis is performed on this system once the stiffness properties of the graphite sealant is experimentally determined in chapter 5. The frequency response and transient response of the system will be shown.

The model of the boring bar-tool assembly can be seen in Fig. 3.4. The model includes the torsional damper as a stiffness and damper in the lateral mode, effect of the graphite sealant is also seen as a damper and a stiffness and also the effect of the cutter and the workpiece which are taken as stiffness and damper of the system.

In actual case since the boring bar used with the

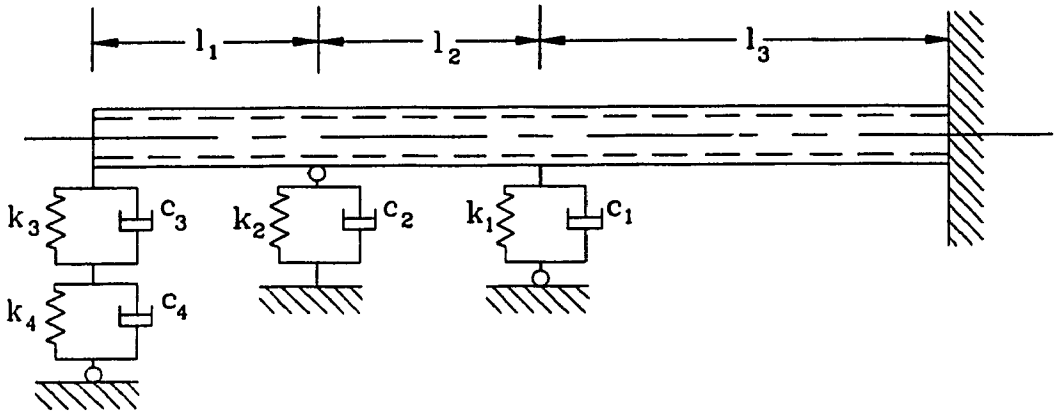

Fig 3.4 Model of the boring bar–cutting tool assembly

machine was not long and slender the operation of the machine without the torsional damper was not critical. Hence the computation of the model in Chapter 5 followed the experimental analysis which was performed without the torsional damper.

CHAPTER 4

STABILITY ANALYSIS OF THE DEEP-HOLE MACHINE

4.1 Stability Analysis

The stability of the deep-hole drilling machine must be studied carefully in order to ensure a good performance of the operation. The bore surface finish totally depends upon the degree of stability the machine maintains. A highly stable machine results in a very well burnished smooth bore, whereas an unstable machine gives a very bad surface finish and a poor operating condition which may eventually lead to a breakage of the tool.

The stability of the machine can be divided into two categories and studied consecutively. The static stability and the dynamic stability. Static stability mainly involves the study of the cutting tool guidance and dynamic stability involves the study of the stability related to the systems dynamic response.

A statically stable system may or may not be dynamically stable, whereas a dynamically stable system ensures static stability. Therefore it is important to have a dynamic stability analysis following a static stability study.

Study of the static stability of the operation helps in the initial design of the tool with its different components. Dynamic stability analysis on the other hand

helps to identify stable zones of operation. First the static stability of the operation will be established.

4.2 Static Stability Analysis

Since the different components affecting the operation in the deep-hole machine are comparatively rigid and well supported the study should be focused mainly on the tool. Stability analysis of the tool should be done in terms of the cutting forces and their balance.

The BTA-solid tool has a single cutter with steps on one side of the tool and pads as shown in Fig 2.1. The cutting force is balanced by the two pads placed at approximately 178° and 276° from the cutting edge, measured in the direction of tool rotation.

Since metal cutting forces fluctuate randomly the stability of the machine should be ensured with a high stability index value so that there will not be any chance of the operation passing into the unstable operation condition. Another factor affecting the fluctuation of guiding pads reactions is the friction coefficient variation.

The cutting force not considering the axial component is balanced by the reactive pad forces. The line of action of this force is moved to the center after the torque is accounted for. The balancing reactive resultant force must be collinear with the cutting force. For the tool to be stable the reactive force must lie well within

the range of the included angle of the pads.

A good stability analysis was given by Pfleghar [41], where he defined the degree of stability (S_d) as the ratio of the sum of all so called holding torques to the sum of tilting torques (eqn. 4.1). These torques consider individual pad as the center of rotation or pivot point.

The holding torque is defined as the torque that presses a pad to the bore surface whereas the tilting torque is a tore that tilts the head around a pad in a direction so as to separate the other pad from the bore surface (Fig. 4.1). The degree of stability is given by;

$$S_d = \frac{\Sigma \text{ holding moments}}{\Sigma \text{ tilting moments}} \qquad (4.1)$$

The degree of stability is computed for each pad separately and the smaller of the two is considered as more critical. Based on the above criterion three ranges of stability degrees are identified and they are;

$$S_d > 1 \quad \text{(stable)} \qquad (4.2a)$$

$$S_d = 1 \quad \text{(indifferent)} \qquad (4.2b)$$

$$S_d < 1 \quad \text{(unstable)} \qquad (4.2c)$$

The degree of stability greater than one implies that the reactive resultant pad force will swing between

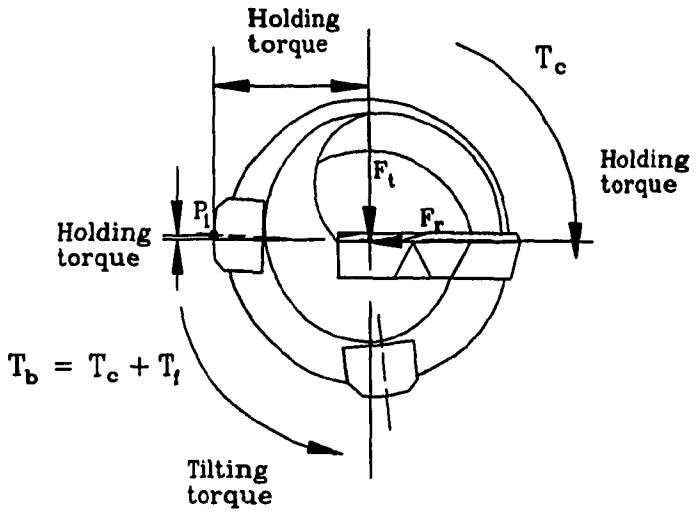

a) Moment about P_1

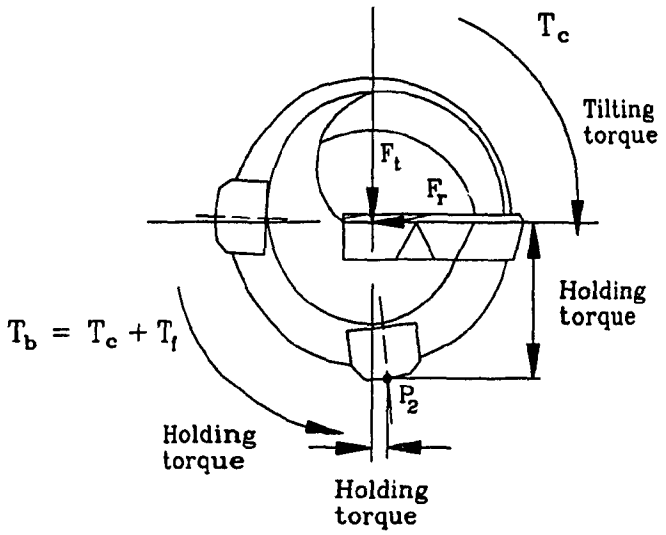

b) Moment about P_2

Fig. 4.1 Stability analysis based on Pfleghar's approach.

the two pads. Indifferent balance having the stability degree equal to unity implies that the reactive resultant force is passing through one of the pads. This is not a good balance as it can easily degenerate into instability under dynamic operating conditions. Finally for the degree of stability less than one the tool is not statically balanced (Fig. 4.2).

Following Pfleghar's stability analysis the BTA-solid tool used in the experiment was found to have a stability degree of approximately 1.6.

4.3 Dynamic Stability Analysis

Study of the dynamic stability of the cutting operation is a very important one. Even though the BTA-solid boring tool is found to be a statically stable tool, there are some machining defects that arise only as a result of the dynamic instability. Therefore one can attain a smooth operation only by identifying this unstable zones of working and avoiding them.

The concept of dynamic stability can best be understood by directly linking the systems natural frequencies in axial torsional and lateral modes to the exciting forces that might be induced and maintained in a regenerative fashion as a result of metal cutting force fluctuation and profile of surface being cut. As seen previously, metal cutting forces are inherently random in nature. In most cutting operations, where the new surface

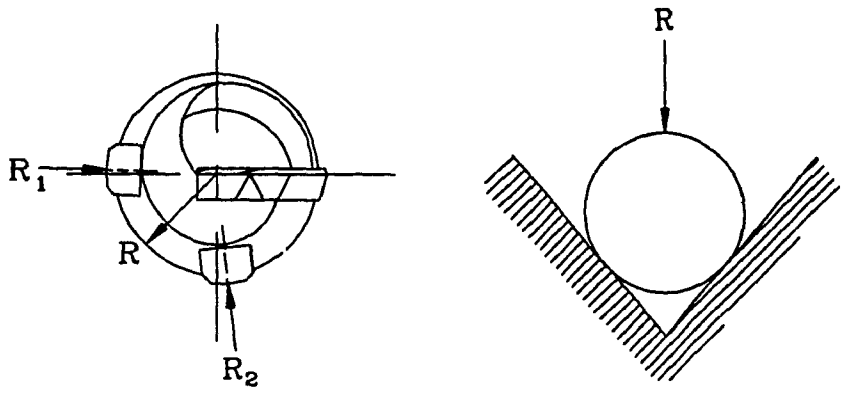

a) Stable balance

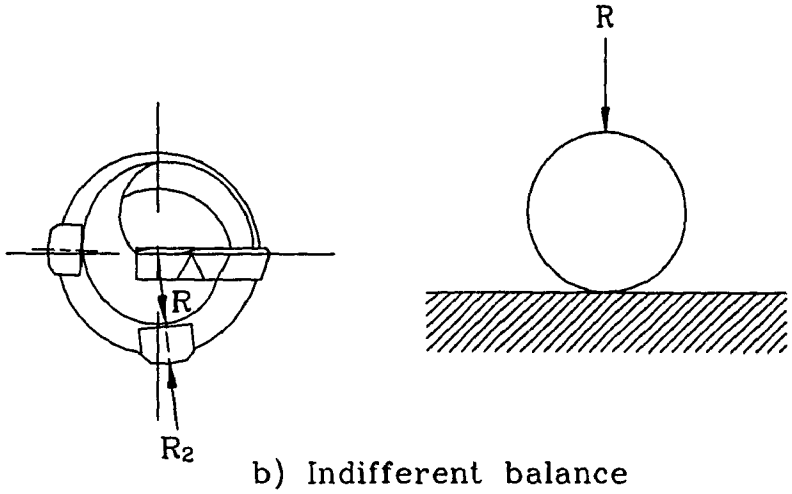

b) Indifferent balance

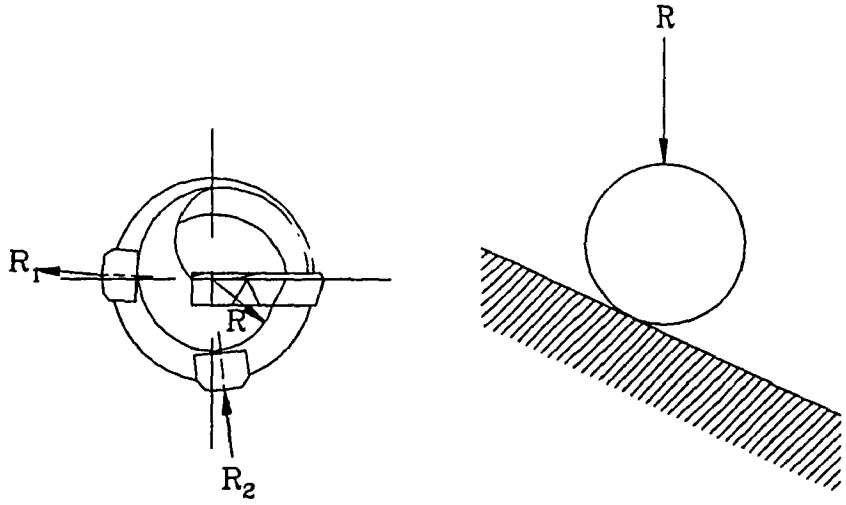

c) Unstable balance

Fig. 4.2 Balance as explained by Pfleghar.

to be cut is the previously machined profile, there is a periodic force component which is dependent on the profile of the surface.

The periodic force component is a regenerative one with a phase difference in the period for every revolution of cut. This is due to the phase lag in the oscillation of the depth of cut of the surface being machined from the currently generated surface, as shown in Fig. 4.3.

In BTA deep-hole machining the geometry of the surface profile to be cut is oriented in such a way that all the three force components and torque come into picture. The tendency of the random cutting force component is to create a surface profile resulting in a regeneratively maintained periodic force component. This type of periodic component is dictated by the dominating stiffness-profile combination, i.e. the direction with the least stiffness for creating a wavy surface profile.

4.3.1 Axial Stiffness

The system's axial stiffness can be considered as the stiffness of the boring bar-tool assembly stiffness and spindle-workpiece assembly stiffness. Due to the relatively short workpiece and high rigidity of the spindle one can assume the axial stiffness of the spindle-workpiece assembly to be infinite. Therefore the axial stiffness of the boring bar-tool assembly is only considered.

The random component of the cutting force can be

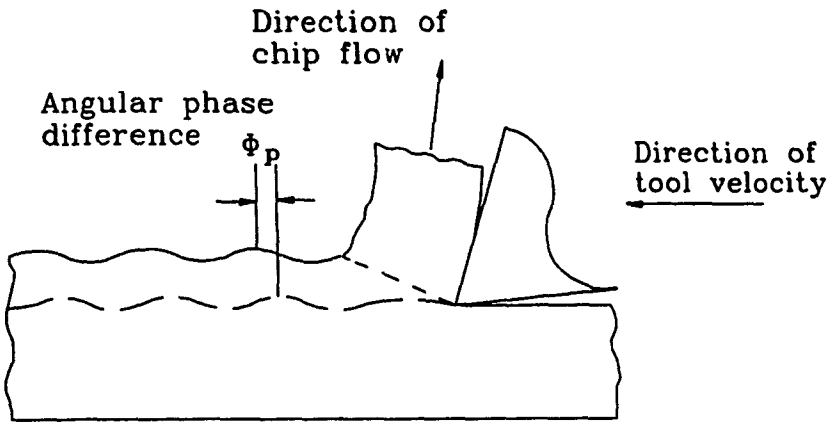

a) Phase difference between machined surfaces

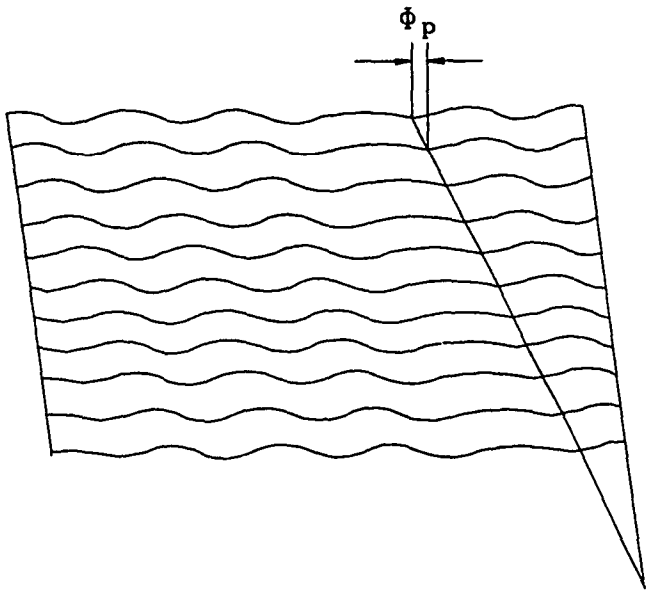

b) Surface profile due to phase difference of previously machined surface

Fig. 4.3 The surface pattern as a result of chatter in machining operations

considered as an exciting input to the system. When the system is axially excited by an impulse force it will vibrate in all its modes before dying down. Since the amplitude of the first or second mode is comparatively high the tendency will be, to vibrate at its first natural frequency. Hence, whatever surface profile variation occurring in the axial direction due to axial force fluctuation, the system will have a tendency to vibrate near the first few natural frequencies in axial mode.

The boring bar-cutting tool assembly, however, is too stiff in the axial direction to bring about a change in the surface profile for most practical applications. Therefore the axial force component fluctuation is not dominant.

4.3.2 Torsional Stiffness

The torsional stiffness of both the assemblies of the spindle-workpiece and boring bar-cutting tool are critical. But since the boring bar-tool assembly is of comparatively low stiffness, one can safely neglect the spindle-workpiece assembly and concentrate on the latter.

The conditions of the boring bar-tool assembly in torsional mode is critical as it involves angular oscillation combined with axial feed. As in the case of axial vibration the exciting force due to randomly varying cutting force component is responsible for the system's torsional vibration. Once the system is excited in

torsional mode it vibrates predominantly near one of its first few natural frequencies. During half of the cycle of vibration the cutter cuts little or no metal because of the angular oscillation direction being opposite the rotary motion of the boring bar-tool assembly. For the remaining half, the cutter cuts more than the nominal depth mainly because the axial feed is maintained constant even when the cutter was in the first half of the cycle.

Therefore the torsional mode of vibration combined with the axial feed motion is a critical phenomenon. This condition might lead to chatter of the system which leads to a deterioration of the tool and its eventual breakage. It depends upon the closeness of the frequency of the periodic force component to the natural frequency of the boring bar-cutting tool assembly in torsional mode. Torsional chatter in the deep-hole machine can be identified by the sharp whistling noise it makes while machining.

Chatter normally occurring in torsional direction, however does not affect the surface finish of the bore except for deterioration of the tool. Most of the surface defects reported have repetitive patterns that are odd numbers per revolution and the frequency of lobe occurrence is too low, as compared to the natural frequency in torsional mode.

4.3.3 Lateral Stiffness

The lateral stiffness also depends on the assemblies of spindle-workpiece and boring bar-tool. As in the previous cases, since the dominant assembly affecting the surface finish of the workpiece is the boring bar-cutting tool assembly, only it will be studied. Another factor for concentrating on this assembly is the orientation of the cutting edge with respect to the boring bar-tool assembly, i.e. whatever input is given to the system in lateral mode as a result of the cutting force fluctuation or surface profile variation, it will be in a fixed direction relative to the boring bar-cutting tool assembly.

The response of the system in lateral mode due to excitation at the tool tip is complex to analyze as it is difficult to model the end conditions at the tool tip exactly. On the side of the cutting edge there is stiffness due to the cutting force while, diametrically opposite, on the side of the trailing pad there is stiffness due to the burnishing action. These stiffnesses were analytically modeled in chapter three. The model was simplified by assuming the stiffness on the pad side to be comparatively too big to affect the performance of the boring bar-tool assembly.

Lateral excitation results in the response of the boring bar-tool assembly, at all its lateral natural frequencies. However the first few modes are dominant enough to show a pronounced effect on the surface of the

bore. This phenomenon may be maintained in a regenerative fashion or may die down depending upon operating conditions and workpiece material.

4.3.4 Multi-Lobe Formation or Spiralling

The concept of multi-lobe formation can best be explained by taking the bored surface finish and magnifying the roundness error generated. If the bore has a tendency to deviate from absolute roundness in lobe like fashion regeneratively, then the phenomenon of spiralling is said to occur. It usually has some lead angle along the length of the workpiece.

Multi-lobe formation occurs as a result of the relative positions of the cutting edge and pads. While machining metal using defective tools, it is not uncommon to come across spiralling phenomenon. These defective tools affect the forces on cutters and pads tremendously, thereby altering the effects of pads on the bore surface. The type of defectiveness detrimental in the formation of spiralling is identified experimentally in Chapter 5.

In the case of the BTA-solid tool, the pad playing an important role in controlling the roundness error, is the trailing pad which is the one placed diametrically opposite to the cutter. This is because of its location. If the circle-land tends to cut more on the bore surface, the burnishing effect of the trailing pad is reduced. Similarly if the circle-land tends to cut less the trailing pad will

press on the bore wall resulting in a highly burnished surface (Fig. 4.4).

The effect of the leading pad is not as pronounced as that of the measuring pad with regards to roundness error. However, the roundness error or multi-lobe formation can be directly associated with the circle-land, trailing pad and leading pad location.

The systems response to the impulsive excitation force at the cutting edge will be in all its harmonics. But the dominant one will be the first mode, ar[illegible] some favorable instances the second one could dominat[illegible]ever, the response of the system is critical only until spiralling pattern is generated.

The geometry of the BTA-solid boring tool shows that the number of multi-lobes formed can only be in odd values. It can be compared to the ordinary twist drill where the corner formation is only in odd values [22,23]. Cronjäger et al [28] have shown the mechanism by which number of lobes has to be odd. The number of times the tool fluctuates per rotation has to be equally spaced between lobes formed. Fig. 4.5 gives a good explanation why even numbered corners cannot occur for this particular tool.

A typical characteristics of this type of multi-lobe formation is that the lobes are visible to the naked eye. This is mainly because the surface cut deep by the circle-land does not get a chance to be burnished well while both pads are riding over this surface. The sole

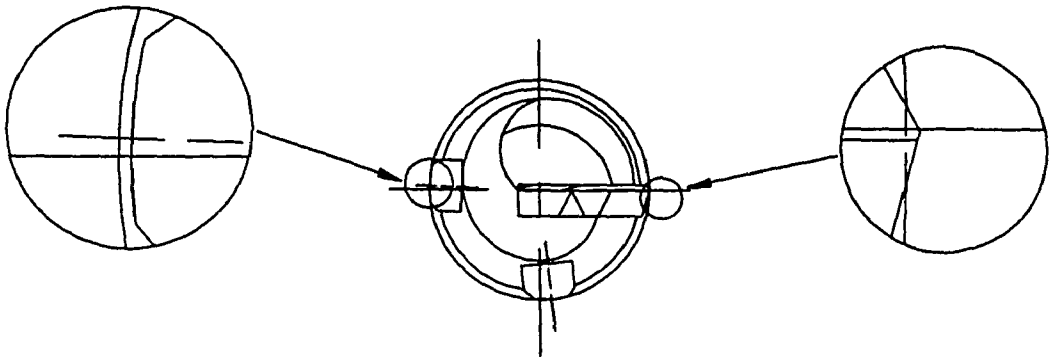

a) Overcut

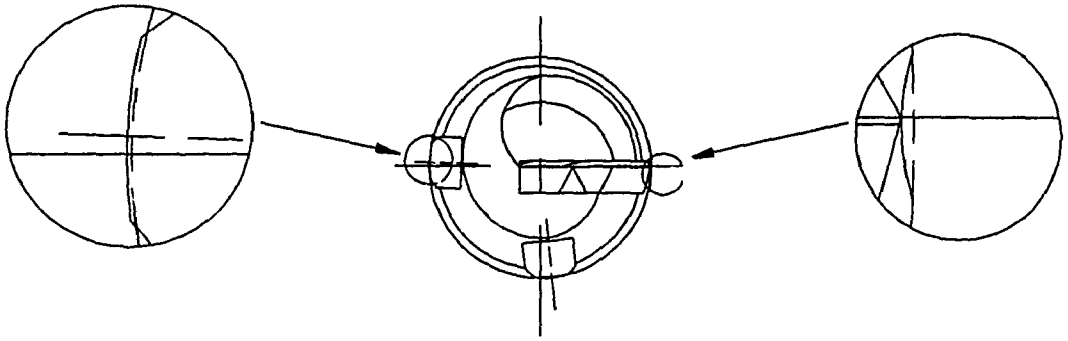

b) Undercut

Fig. 4.4 The phenomena of overcut and undercut in the BTA–solid tool.

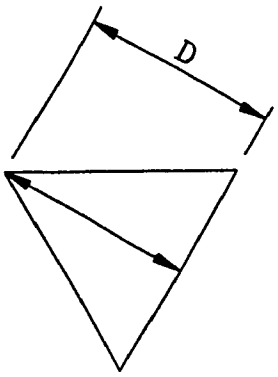

3 Lobes

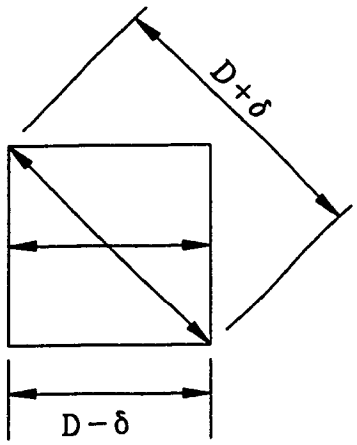

4 Lobes

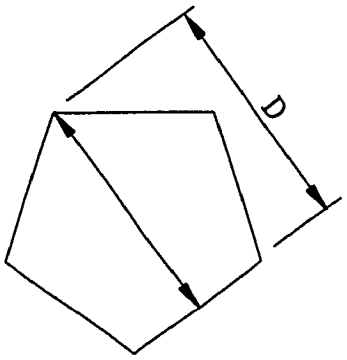

5 Lobes

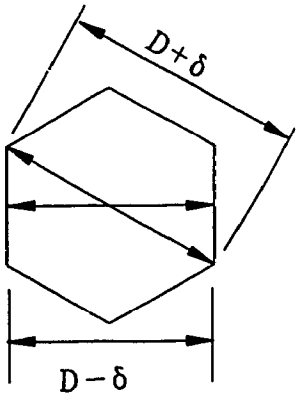

6 Lobes

a) Odd number of lobes

b) Even number of lobes

Fig. 4.5 Multi-corner formation in BTA-solid drilling tool.

reason for the lobe formation is the circle-land being guided into the bore surface by the pivoting action of the leading pad.

The circle-land position with respect to the circumference should be the nominal size of the tool. If it is not it will result in its digging into the surface producing oversize or it will in its recess producing undersize of the hole.

The experimental study of the spiralling phenomenon has been done for different materials at different operating conditions. The principles by which spiralling is formed are analyzed and discussed in detail and followed by the experimental justification in the next chapter.

CHAPTER 5

EXPERIMENTAL STABILITY EXAMINATION OF BTA-SOLID TOOL SYSTEM

5.1 Dynamic Stability Assessment

Dynamic stability analysis of the BTA-solid drilling tool was done experimentally on the machine modeled mathematically in Chapter 3. Since the main aim of the experiment was to correctly identify spiralling, favorable conditions were chosen so that it can be induced by machining at speeds and feeds giving rise to it and also by using defective tools.

The experiments were performed on the Schaerer lathe which was retrofit to a deep-hole boring machine, by introducing a pressure head and a drive unit along with the coolant filtering and circulating system. This modified machine has a length of 4m and the capability of machining workpieces as long as 1m and having an internal diameter of up to 50mm.

The experimental procedure comprises three stages. The first one is identification of the natural frequencies of the boring bar-tool assembly, because it is critical to the operation of the machine, the second one is the machining of different specimens using BTA-solid tools, at speeds corresponding to critical values of the system's frequency i.e. the natural frequency an odd multiple of the relative speed of workpiece and tool and the third one is

machining the specimens using a defective tool with its circle-land slightly bigger than nominal size. To assert the validity of the experiment different materials were used as the workpiece, and the experiment repeated a number of times for repeatability assessment.

5.1.1 Boring Bar Lateral Natural Frequency Determination

The boring bar is fixed to the drive unit and passes through the pressure head. Since the exact cutting conditions are required for modelling of the system the tool was made to dig into the workpiece an amount equal to the feed. A small attachment device was made from aluminum to hold the accelerometer in place on the boring bar. This accelerometer was connected to a charge amplifier which was then connected to a personal computer with the help of an analog to digital converter (Fig. 5.1).

The main purpose of this set up was to determine the natural frequencies of the system. Hence the transient response of the system was collected at a sampling rate of 400 data per second. This was done because of the relationship of the Nyquist frequency to the sampling rate, i.e. the maximum frequency of interest is less than 200Hz.

After obtaining the well sampled data in time domain, discrete Fourier transform was performed to obtain the data in frequency domain. Finally the power spectral density was calculated from the Fourier transform and then plotted against frequency.

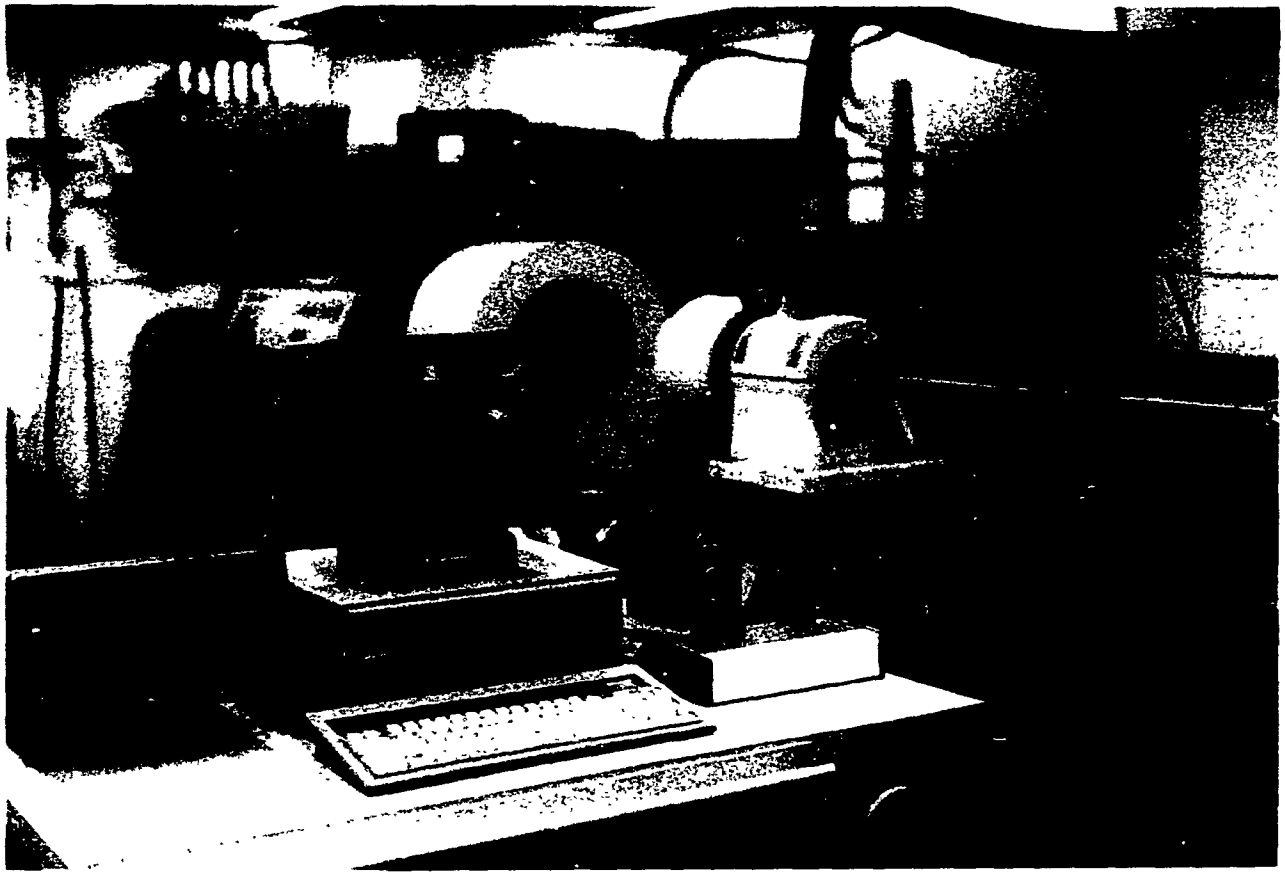

Fig. 5.1 Experimental setup for data acquisition

The Fourier transform for the discrete data, which gives a good insight into the general behavior of the system in frequency domain, was calculated using the following equation;

$$X(f) = h\sum_{n=0}^{N-1} x(nh)e^{-i2\pi fnh} \qquad (5.1)$$

where

N = number of relevant data collected

x(nh) = discrete data sampled at an interval h

f = frequency

Performing eqn (5.1) provides the Fourier transform as shown

$$X_k = \frac{X(f_k)}{h} = \sum_{n=0}^{N-1} x(nh)e^{(-i2\pi kn/N)} \qquad (5.2)$$

where

$f_k = kf = \frac{k}{Nh}$

k = 0,1,2,...,200-1

The Fourier spectrum is a plot of the coefficients of the Fourier series against frequency f. The absolute values of X_k are generally plotted.

The power spectral density function is a means of

studying the overall frequency distribution. The plot of this function vs frequency establishes the frequency composition of the data, which bears an important relationship to the basic characteristics of the physical system involved.

The power spectral density for the discrete data is given by the following equation;

$$P(f_k) = \frac{2h}{N}|X_k|^2 \qquad (5.3)$$

Figs. 5.2-4 give a plot of the power spectral density against frequency, computed using MATLAB software, for the boring bar at different penetration into the workpiece, namely at 25mm, 150mm, and 300mm respectively. From the plots the frequency distribution can be obtained and its variation along the length of the workpiece can be observed as given in Fig. 5.5a.

The determination of the natural frequency experimentally helps in identifying the stiffness characteristics of the graphite sealant between the boring bar and the pressure head. This stiffness quantity can be estimated from the plot showing different natural frequencies vs stiffness values Fig. 5.5b [46]. After giving an equivalent value to the stiffness provided the sealant frequency variation is plotted for the entire tool penetration of 600mm as shown in Fig. 5.6. The lateral natural frequency distribution of the boring bar tool

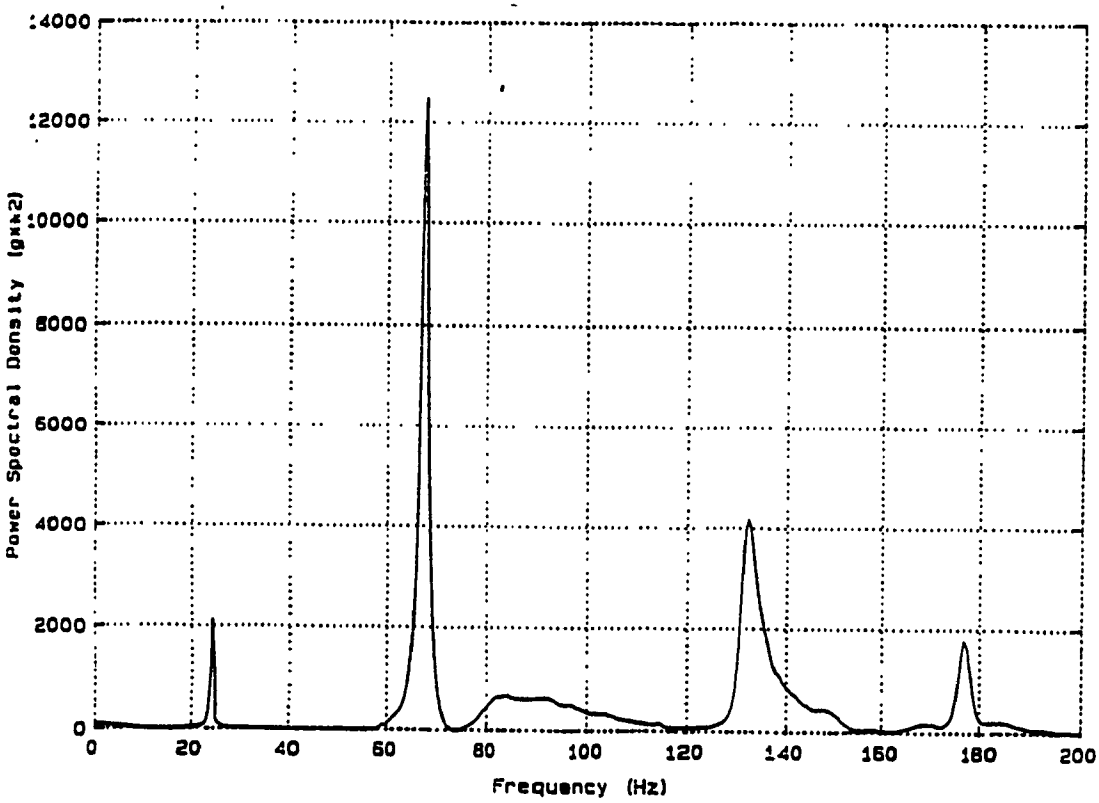

Fig. 5.2 Power spectral density for first position

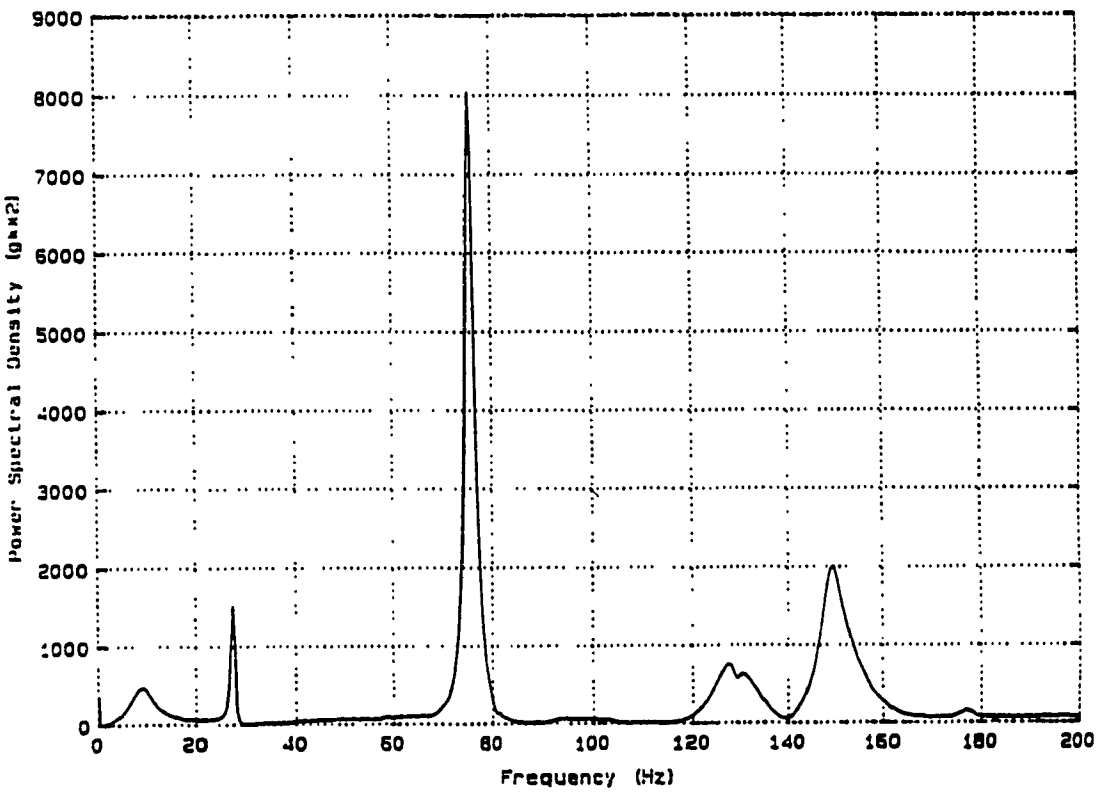

Fig. 5.3 Power spectral density for second position

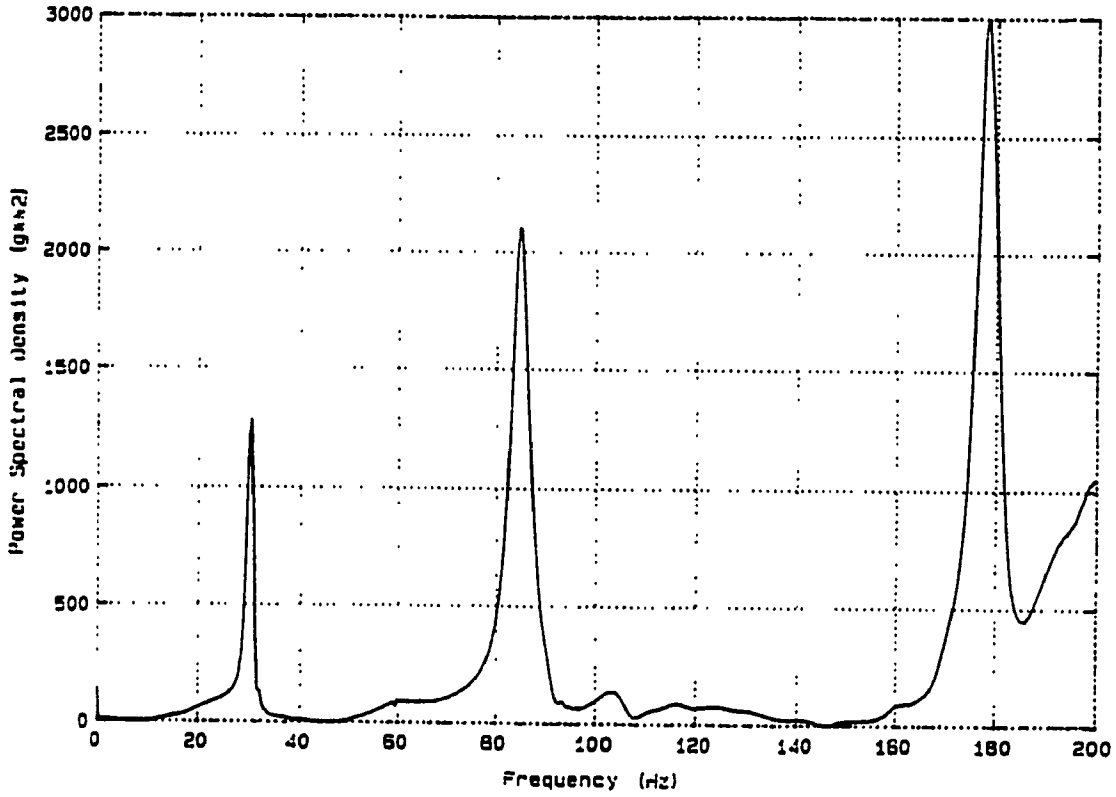

Fig. 5.4 Power spectral density for third position

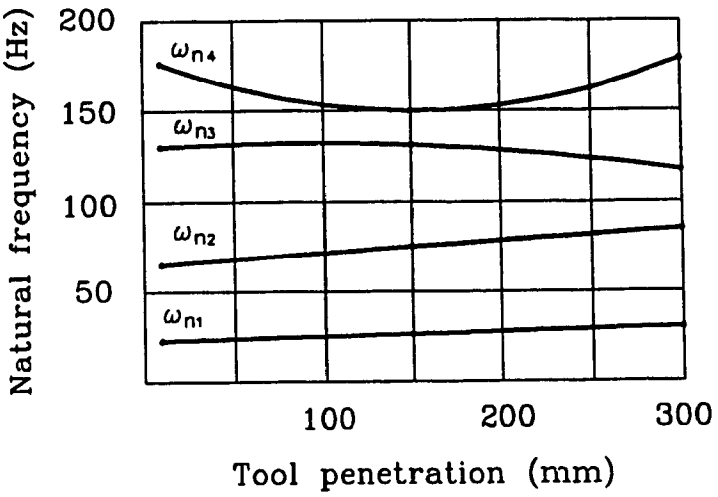

a) Natural frequency variation

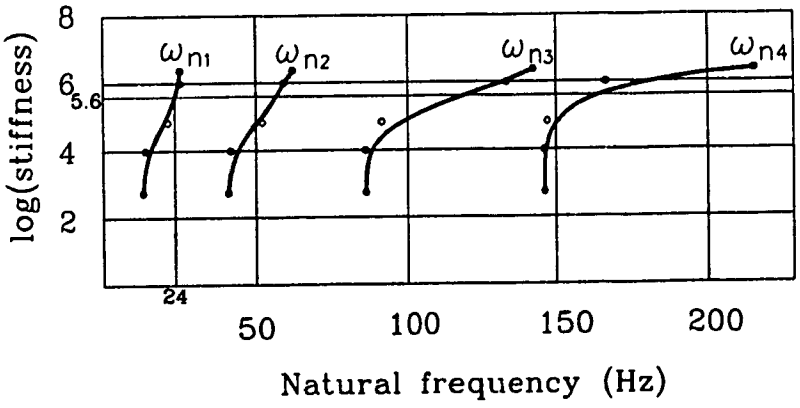

b) Stiffness vs natural frequency

Fig. 5.5 Lateral natural frequency for different stiffness values

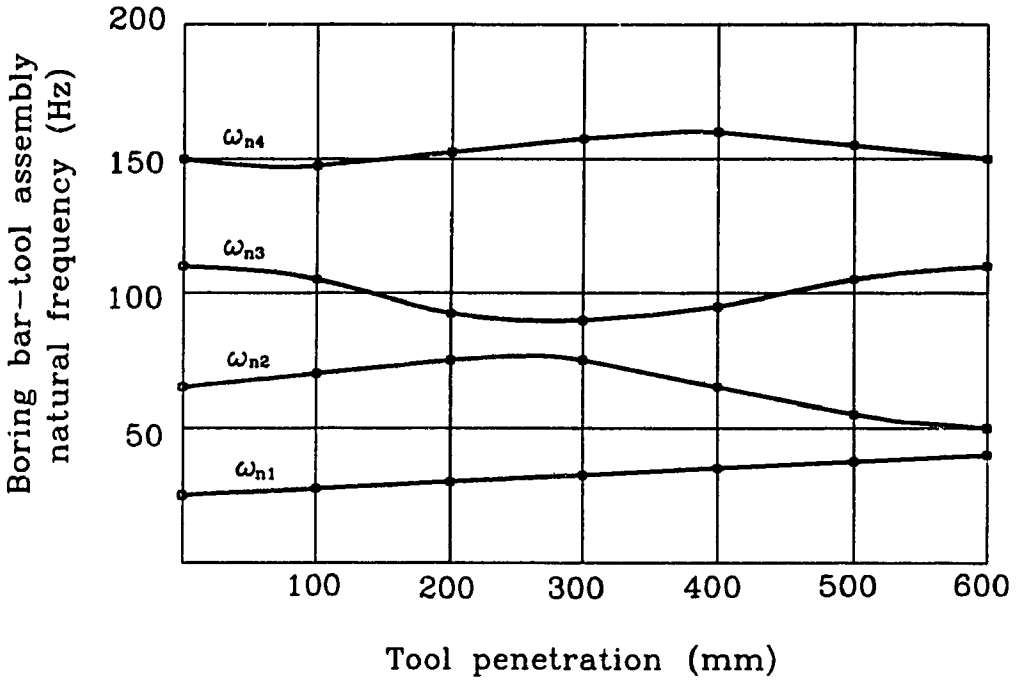

Fig. 5.6 Lateral natural frequency for deeper tool penetrat

assembly was found using the ANSYS finite element package available on the VAX 8530 [48].

The lateral natural frequency plays a significant role in the formation of spiralling. This was the main reason why its accurate determination was essential in the analysis of multi-lobs formation.

5.1.2 Formation of Spiralling Under Operating Conditions

It is common to come across odd numbered lobes or multi-lobes under unstable drilling conditions, using the twist drill. The same is true for deep-hole boring tools. The geometry of the BTA deep-hole drilling tool is such that it gives odd numbered lobes due to the location of the cutter, the circle-land and pad being opposite each other.

The Phenomenon of spiralling has been reported by previous researchers such as Sakuma et al [25] and Stockert et al [28]. But the analysis reported by the two researchers was contradictory to each other and none of them have suggested a possible remedy to the problem.

One of the major factors proposed as influencing the formation of spiralling is the position of the circle-land relative to the nominal diameter of the tool. Tools with circle-lands more than 25 to 50μm oversize relative to the leading pad measured from the center have a high chance of yielding spiralling. For this reason an experiment involving a tool with 50μm oversize of circle-land from the center was used to drill all the available materials.

Another factor proposed as influencing the formation of spiralling was the effect of lateral natural frequency. Based on odd number of lobes formation, namely 3, 5 and 7, the experiment was conducted such that one of the major natural frequency namely the 1^{st}, 2^{nd} or 3^{rd} coincided with an odd spiralling frequency per revolution, which is one of the above numbered values (3, 5 or 7) for every turn. This implies that the spiralling frequency (number of lobes per revolution times number of revolutions per second) coincides with the lateral natural frequency.

The following equation gives a relationship between the natural frequency, relative rpm and number of lobes formed.

$$\eta_r = \frac{60 \cdot f_n}{n_l} \qquad (5.4)$$

where

f_n = lateral natural frequency (hz)

n_l = number of lobes formed

η_r = relative velocity in revolution per minute

Figure 5.7a shows the critical frequency distribution for different rpms.

While actually performing the experiment, there were a number of limiting factors:

a) The surface cutting speed had to be adjusted

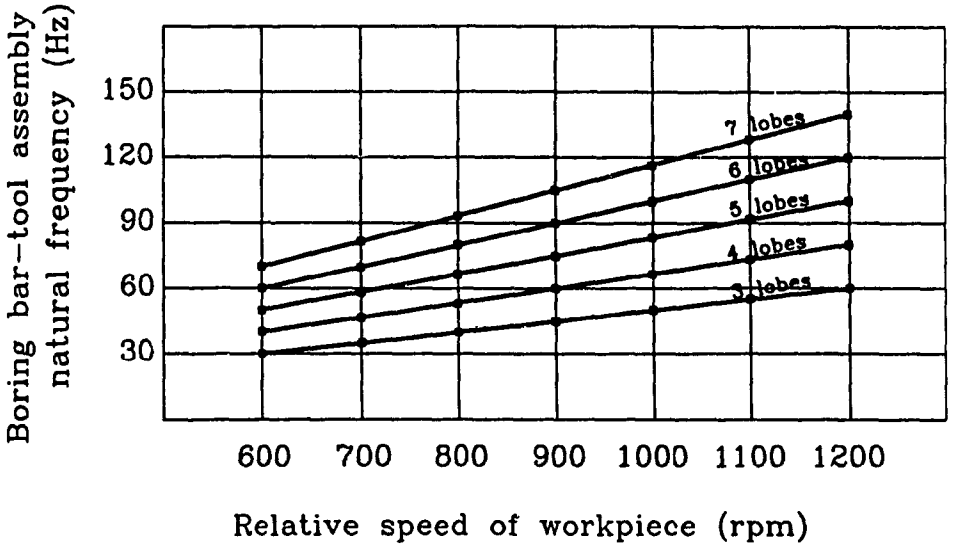

a) Multi–lobes formation corresponding to different speeds and frequencies.

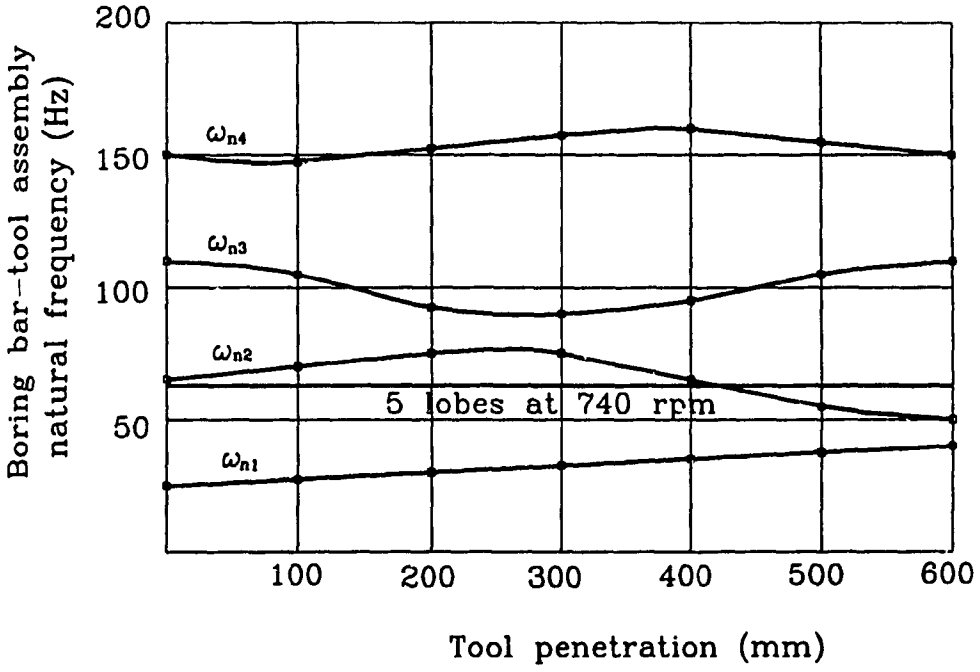

b) Formation of spiralling corresponding to 740 rpm and five lobes.

Fig. 5.7 Critical frequency distribution

within a range so that cutting is stable.

b) The boring bar had to be fixed in order to take response of the system while it was machining.

c) Available speed for the workpiece changes discretely so that finding a match for the frequency with respect to the number of turns per minute was difficult.

Restricted by the above conditions the machining was done at the three available speeds such that the first few natural frequencies coincided with a possible number of lobes, including even and odd values as shown in fig. 5.7a.

The natural frequency distribution of the boring bar in lateral mode is plotted as shown in figs. 5.7b, 5.8a and b in relation with five number of lobes formation for the available speed. Table 5.1 gives the amount, the natural frequency should be, in order to obtain the number of lobes shown on the left side. The rpm of the workpiece is given in three steps as it is the available recommended value of operation in the range, i.e., circle-land speed between 60m/min and 100m/min for the materials used [32].

Five types of workpiece materials were available, four of them are of similar nature, in that their machinability rating is comparatively low, whereas the the fifth one has lead added to it to increase its machinability to 160%. The workpiece materials used are as given in table 5.2.

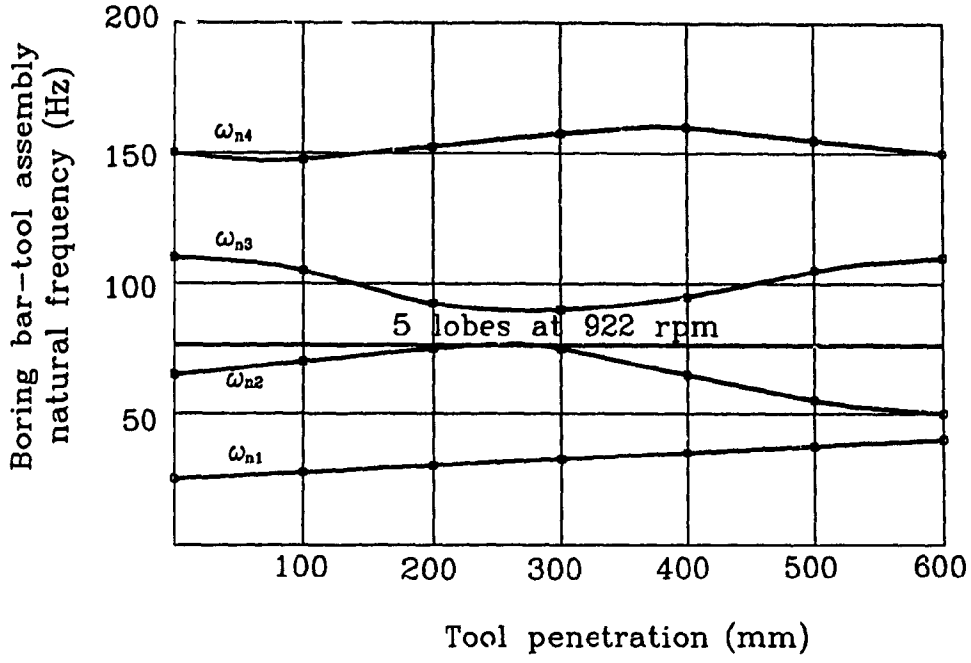

a) Formation of spiralling corresponding to 922 rpm and 5 lobes

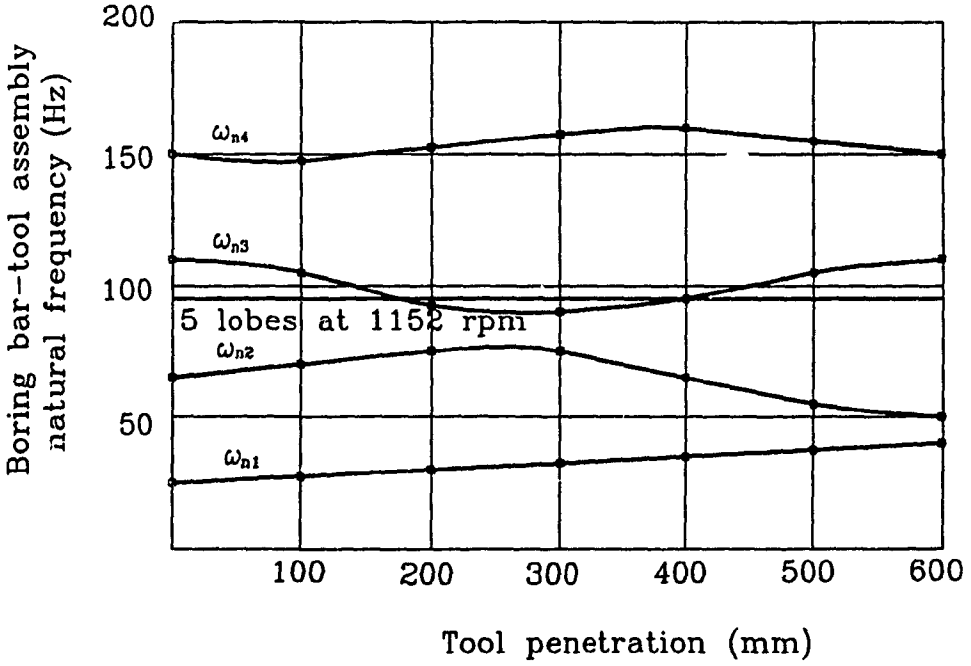

b) Formation of spiralling corresponding to 1152 rpm and 5 lobes

Fig. 5.8 Critical frequency distribution for higher speeds

Table 5.1. Value of natural frequency for the given lobes at the available rpm.

No. of lobes	workpiece speed (rpm)		
	740	922	1152
3	37	46	58
5	62	77	96
7	86	108	134

All the above specimens were cut at 0.60m length and prepared for machining by chamfering at the ends so that they fit on the reception plate of the pressure head. The outside diameter of the workpiece was 31.75mm and the inside diameter of the hole was 25.4mm.

After trying the three available rpms on the lathe at variable feed spiralling was formed only in 5 lobes, at a particular speed (740rpm), for a limited length while using slightly worn tools. The length was dictated by the natural frequency variation. This means as long as the natural frequency was coinciding with the frequency of the lobe occurrence the phenomenon of multi-lobe formation was maintained. But once this frequency has changed due to penetration of the tool-boring bar assembly the lobe formation was terminated. Spiralling was being formed for all the materials except the AISI C12L14. This is mainly because the material has a very good machinability rating (160%), implying that the random component of cutting is

Table 5.2 Workpiece materials and their properties.

Steel Designation	Yield Strength N/mm^2	Average Ultimate Strength N/mm^2	Application
ASTM A36	250	480	general purpose structural quality steel used for tie rods, brackets, frames, etc.
AISI C1020	230	425	general purpose machinery steel used for bolts or hammer forgings.
AISI C12L14	465	540	for high speed production of bolts, nuts, fasteners, etc.
AISI C1045	425	615	medium carbon steel used for axles, shafts, bolts, etc.
AISI C1095	515	1015	high carbon steel used extensively for making springs.

not high enough to induce vibration. Spiralling formed due to lateral bending frequency was occurring even when the length of the workpiece was reduced by half, supporting the

theory explained in Chapter 3, i.e. the frequency of the boring bar-tool assembly is critical. Also the tool condition affected the formation of spiralling a great deal. Worn out tools used yielded spiralling at the given speed irrespective of the material and feed, whereas a reground tool was not giving spiralling in four of the five materials used and even in the fifth one it gave spiralling at low feeds only. Again the reason for this being that this material was the one with the least machinability index of 55%.

The response of the system measured during the occurrence of spiralling was analyzed and plotted to give the power spectral density as shown in Fig. 5.9. The spiral plot done using the Talyrond roundness measuring device for holes with spiralling is as given in Fig. 5.10.

The other mechanism by which spiralling was generated, was while machining with a tool having its circle-land oversize by about 50μm relative to the two pads around the circumference of the tool. In this case spiralling was formed at all operating speeds for all the workpiece materials except one (C12L14) and the lobes were along the whole length of the specimen. This fact showed that the spiralling in this case is not frequency dependent as in the first case.

These occurrences lead to an investigation in analyzing the factors affecting the formation of spiralling in detail.

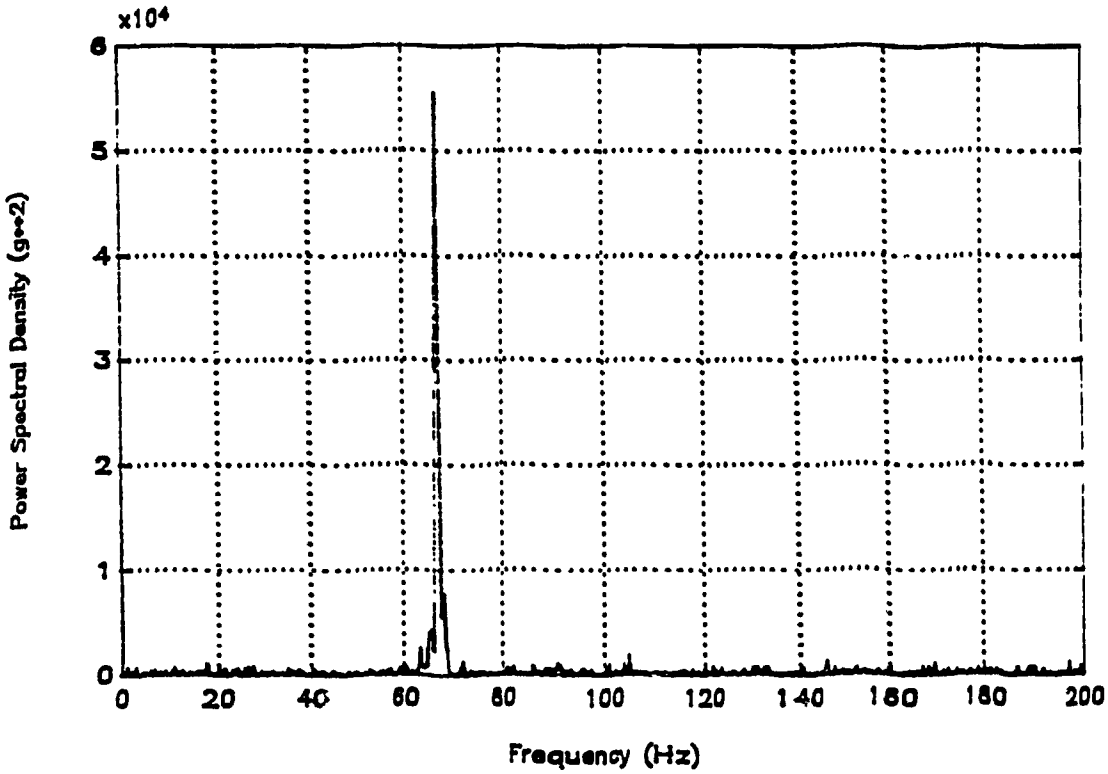

Fig. 5.9 Power spectral density of spiralling

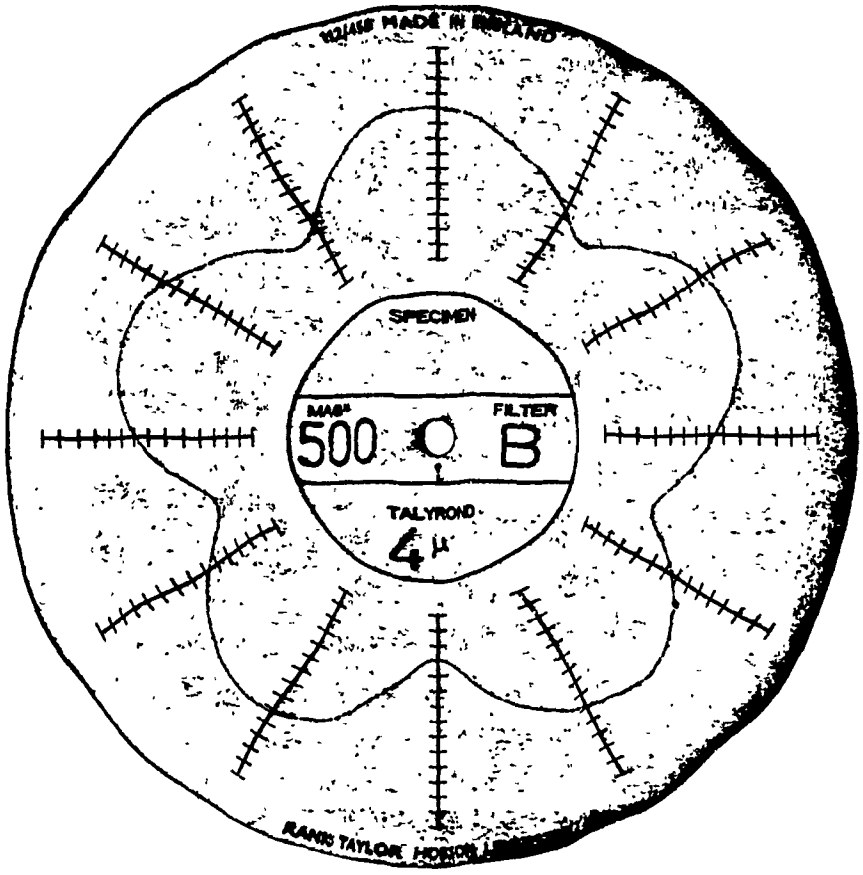

Fig. 5.10 Polar plot of multi-lobe hole

5.1.3 Factors Affecting Spiralling

Spiralling in its entirety is a very complex phenomenon. While conducting the experiment, there were a number of factors observed that affected spiralling.

1) Tool bluntness

2) Position of pads

3) The relative position of circle-land on the circumference.

4) The coincidence of the natural bending frequency with appropriate number of lobes (five in BTA-solid boring tool).

5) Workpiece material properties.

5.1.3.1 Tool Bluntness

Bluntness of the cutting edges affects the cutting action of the tool a great deal. The major effect is that the cutting force increases. This implies that the steady state, periodic and random component of the cutting force increase proportionally. Hence if the workpiece is rotating at an angular speed which equates the spiral frequency to a dominant natural frequency that is varying five times every rotation, it could lead to spiralling.

In the experiment conducted a freshly ground tool that was stable degenerated into giving spiralling only after about the first fifty percent of its life, provided the other conditions affecting the formation of spiralling, especially coincidence of lateral natural frequency with

spiralling frequency, were met.

5.1.3.2 Location of Pads

In BTA tools the relative location of the pads and cutter is of great importance. The number of lobes formed are dictated by the relative position of the circle-land and pads. Since spiralling occurs when tool pivots about the leading pad forcing the circle-land to dig deep into the workpiece, the pad opposite to the circle-land will not burnish the surface because it is lifted. While this occurs the leading pad acts as a moving pivot point rolling along the bored surface.

Measurement of the angle between the circle-land and leading edge of the leading pad indicates that the value is approximately one fifth of 360^{0} circle. This supports the idea that spiralling occurs as a result of a pivoting action on the leading pad forcing the circle-land to dig into the bore surface.

5.1.3.3 Location of Circle-Land

The relative location of the circle-land with respect to the pads is important in the formation of spiralling. The circle-land should be on the circumference of the circle formed by the pads. If the circle-land is a undersize then the bore will result in a smaller dimension (undersize). However if the circle-land is oversize then there is a higher possibility of spiralling as it will dig

into the workpiece on and off continuously.

Spiralling formed as a result of the circle-land being oversize was persistent for the entire length of the hole and degenerated into spiralling irrespective of the relative speed used.

5.1.3.4 Lateral Natural Frequency of Boring Bar

The lateral natural frequency of the boring bar-tool assembly affects the cutting if it coincides with five cycles per revolution. The reason being that spiralling in BTA-solid tools occurs only in five lobes due to the geometry of pads and cutter location.

Performing deep-hole drilling at a certain speed where the lateral natural frequency coincides with five cycles for every revolution will result in the bar vibrating at its natural frequency for the duration the coincidence lasts. This implies that the chance of spiralling is increased when this occurs.

5.1.3.5 Workpiece Material

The workpiece material affects the formation of spiralling a great deal. If the material is easy to cut and random component of the cutting force is comparatively low then the chances for the formation of spiralling is reduced. However, if the material is not easy to machine by virtue of its mechanical properties then it gives one of the favorable cutting conditions for the formation of

spiralling.

5.1.4 Mechanism for the Occurrence of Spiralling

The mechanism by which spiralling formation occurs is primarily the same, even though there are two major causes initiating it. One of the factors is the effect of natural frequency while the other factor is the effect of circle-land. These two can be identified by the length of the spiral along which it occurs. If the spiralling is as a result of the circle-land being oversize then spiralling occurs along the entire length of the hole, whereas if it is due to the lateral natural frequency then it will be there for only a short depth until the change in natural frequency, due to tool penetration, occurs.

Formation of spiralling as a result of the lateral natural frequency can be explained as follows:

1) The random component of the force on the trailing pad has to be high enough to induce excessively high load fluctuation on the cutter along the circle-land such that the boring bar-tool assembly is excited at one of its modes. Despite the fact that new tools have a comparatively low reaction force on th trailing pad, Griffith explains that this is not the case for worn tools. The force on the trailing pad for worn out tools was experimentally found to be almost equal to that on the leading pad [47]. Therefore this explains the reason why spiralling is predominantly occurring for worn tools.

2) The excitation in the trailing pad-circle-land direction tends to bring excessively high loads on the leading pad, as a result of an increase in cutting force, causing the trailing pad to be lifted from the surface while the circle-land digs into the bore wall.

3) Due to high forces, the tool tends to tilt around the leading pad in the circle-land direction reducing the load on the trailing pad and cutting deeper into the bore surface.

4) This tilting occurs until the leading pad has passed over the peak as shown in fig 5.11, then the cutter comes back to its original position because of the excessive radial force due to the circle-land digging in.

5) Because of the location of the circle-land and pads this digging in and coming back to its original position of the tool happens 5 times per every revolution. This is the main reason why spiralling formed while using BTA-solid boring tool gives only 5 lobes.

Spirals formed in the hole propagate at some lead angle along the bore length. It was found that the lead angle was inversely proportional to the roundness error, i.e., the lower the roundness error the higher the lead angle, and inversely the higher the roundness error the lower the lead angle. Even though this phenomenon was observed for most drillings the spiral angle cannot be systematically explained and predicted at this level. Hence, if the size of the peak is comparatively high the

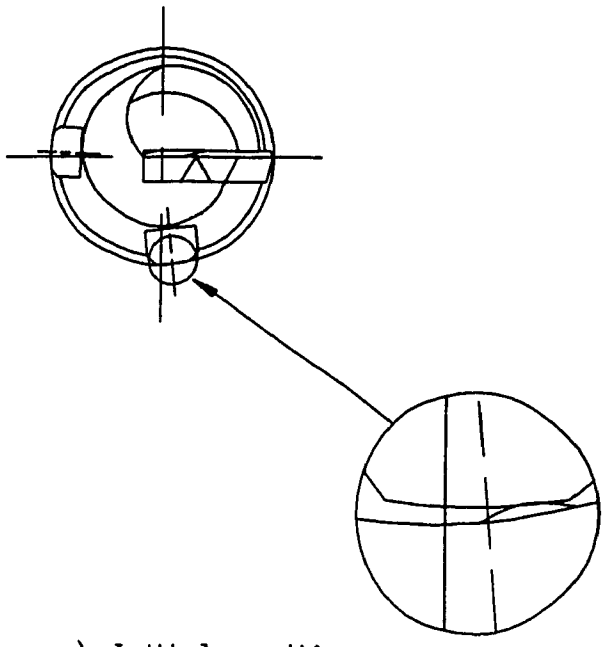

a) Initial position

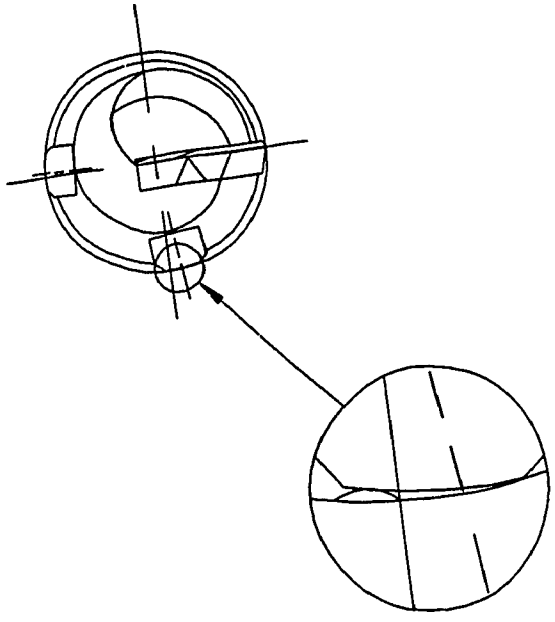

b) Final position

Fig. 5.11 Leading pad orientation while spiralling

phase difference will be very small resulting in a very low lead angle. If the peak is comparatively small the phase shift will be high resulting in a high lead angle.

The BTA-solid deep-hole boring tool is very stable. In fact according to Pfleghar's stability criterion it is the one with maximum stability index as compared to other BTA tools. However, in dynamic sense the situation is totally different. The friction coefficient which is occurring between the pads and the workpiece is assumed to be constant and it is normally given values between 0.2 and 0.3. However some researchers have reported friction coefficients as high as 0.6 [47]. Static resultant force direction variation relative to friction coefficient on the different pads has been shown in the second chapter (Fig. 2.6)

Close examination of bored surface frequently gives an irregular cut of the surface at random. No researcher has so far come up with logical explanations, as to why, the above mentioned phenomenon occurs. This could be mainly because of the unpredictability of the Coulomb's friction coefficient. Another possibility not so far mentioned is the stick-slip phenomenon which may occur between the leading pad and the bore surface, instantaneously, as a result of high forces coming on the pad.

In the BTA-solid boring tool the cutter and pads location is such that the forces coming on the leading pad is almost twice as much as that on the trailing pad. From

the equations derived in Chapter 2 relating the different instantaneous forces to the resultant instantaneous force, one can see that the variable component of the forces will also be in this proportion. Considering the random component of the cutting force as the impulse input for the excitation of the boring bar-tool assembly, the transient response of the system can be studied. The transient response of the system dies down in the the first few dominant modes such as the third, second and finally the first. Depending upon the relationship between the lateral natural frequency and spiralling frequency, identified as the product of number of lobes per revolution and number of revolutions per unit time, spiralling occurs at one of the lateral natural modes.

The spiralling occurrence observed for most of the cases formed happened at the second natural frequency of the boring bar-tool assembly (62Hz), and lasted only for a short length of the workpiece, as long as it remained around this region. But right after the lateral natural frequency was altered due to longitudinal travel of the boring bar-tool assembly, the spiralling phenomenon stopped, supporting the theory of bending natural frequency affecting spiralling.

5.1.5 Prevention of Spiralling

The experimental results show that the spiralling phenomenon is a complex one and it needs a number of

factors to be satisfied before it actually begins to occur. The favorable factors leading to spiralling involved the digging of the circle-land into the bore wall (Fig. 5.12).

The circle-land is an essential part of the tool which one cannot avoid. It is responsible for cutting the the correct hole size while drilling. Hence one should come up with a plan to prevent the circle-land from digging into the bore wall more than what it should.

The digging action of the circle-land can be avoided by preventing it from going sideways with the help of guide pads right behind the circle-land. This ensures that the previously cut and burnished surface will prevent it from moving radially outward into the surface of the bore wall.

In this experiment the attempt to prevent spiralling was first made by inserting a guide pad behind the worn out cutter that was yielding spiralling (Fig. 5.13a). The tool was then used to machine under the exact same conditions that resulted in the formation of spiralling. Since the circle-land was prevented from digging into the workpiece, spiralling was avoided in all the specimens. Since the force expected on this pad is relatively small for stable cutting, a comparatively small pad size can be used as shown in the figure.

The next improved tool was a completely modified version and made with a pad at the circle-land (Fig. 5.13b). This tool was used to machine many specimens and satisfactory results were obtained. The polar plot obtained

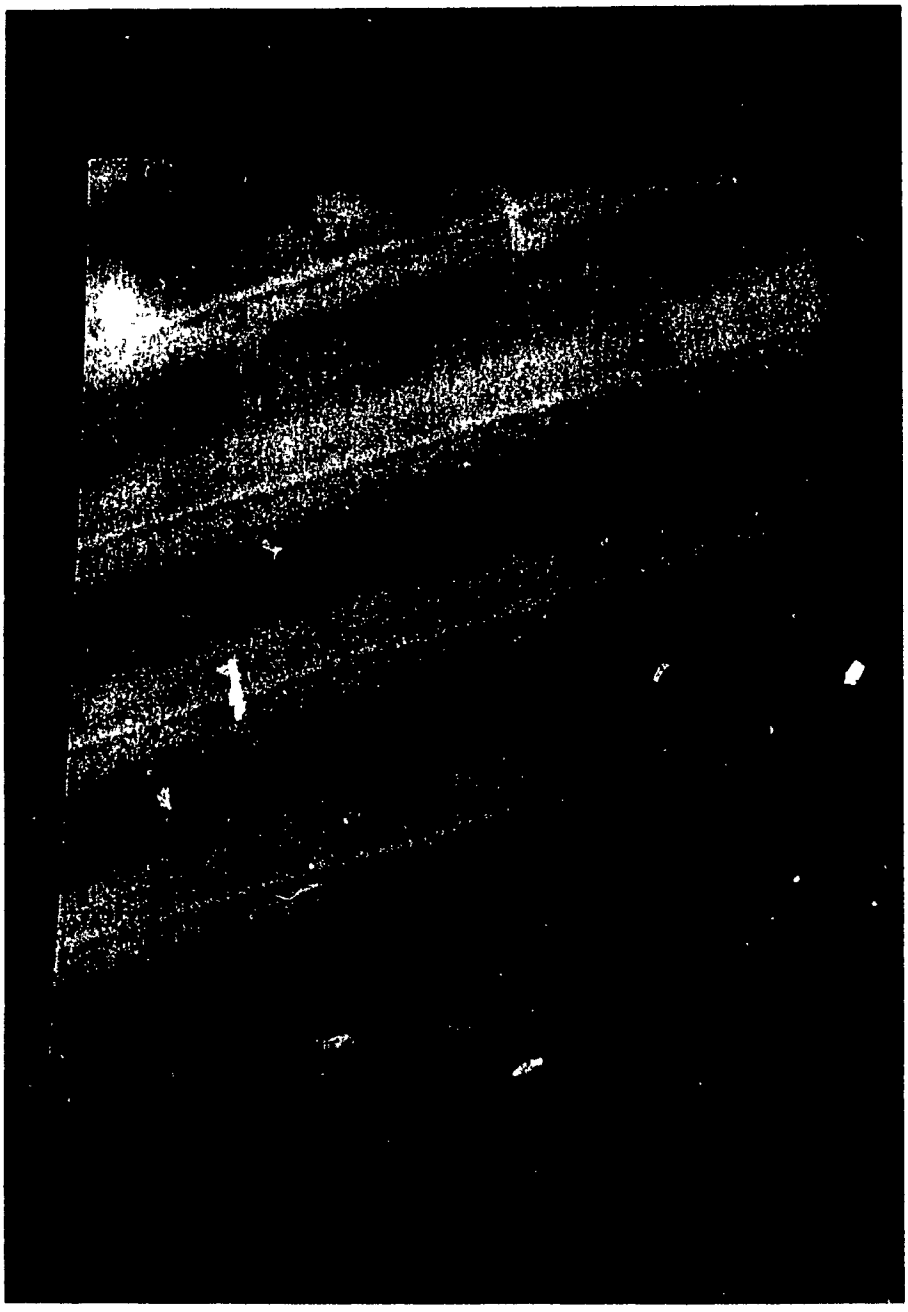

Fig. 5.12 Specimen with spiralling on the surface

a) Pad inserted below circleland

b) Pad ground behind circleland

Fig. 5.13 Picture of modified BTA–solid tools

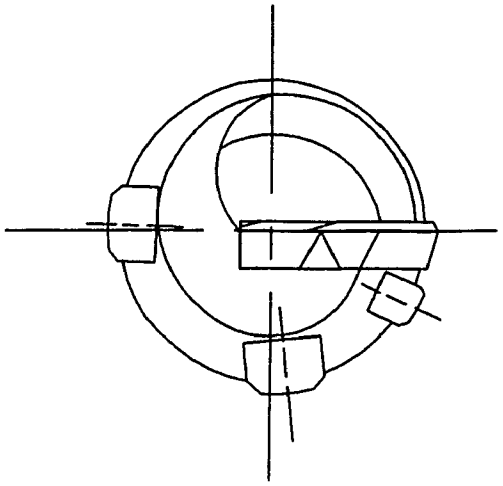

a) Tool with third pad inserted.

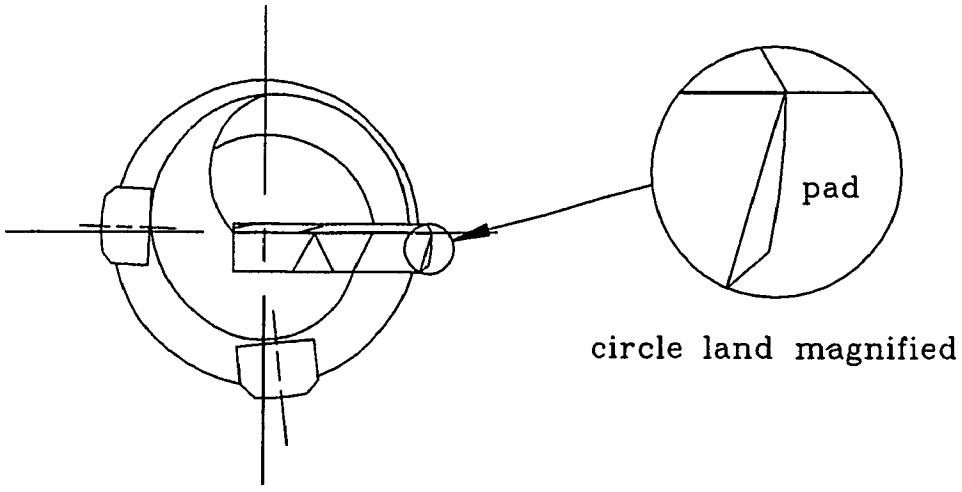

b) Tool with pad ground behind circle land.

Fig. 5.14 Modified BTA-solid tools

using a Talyrond, the roundness error measuring device, given by Fig. 5.14a and b, shows the difference between the holes made by the newly modified tool and the regular BTA-solid boring tool.

In this chapter the deep-hole boring machine system was experimentally tested for dynamic response and the formation of spiralling was identified and explained. The remedies for spiralling prevention were suggested and justified experimentally. The final chapter gives conclusion and recommendation for further research work.

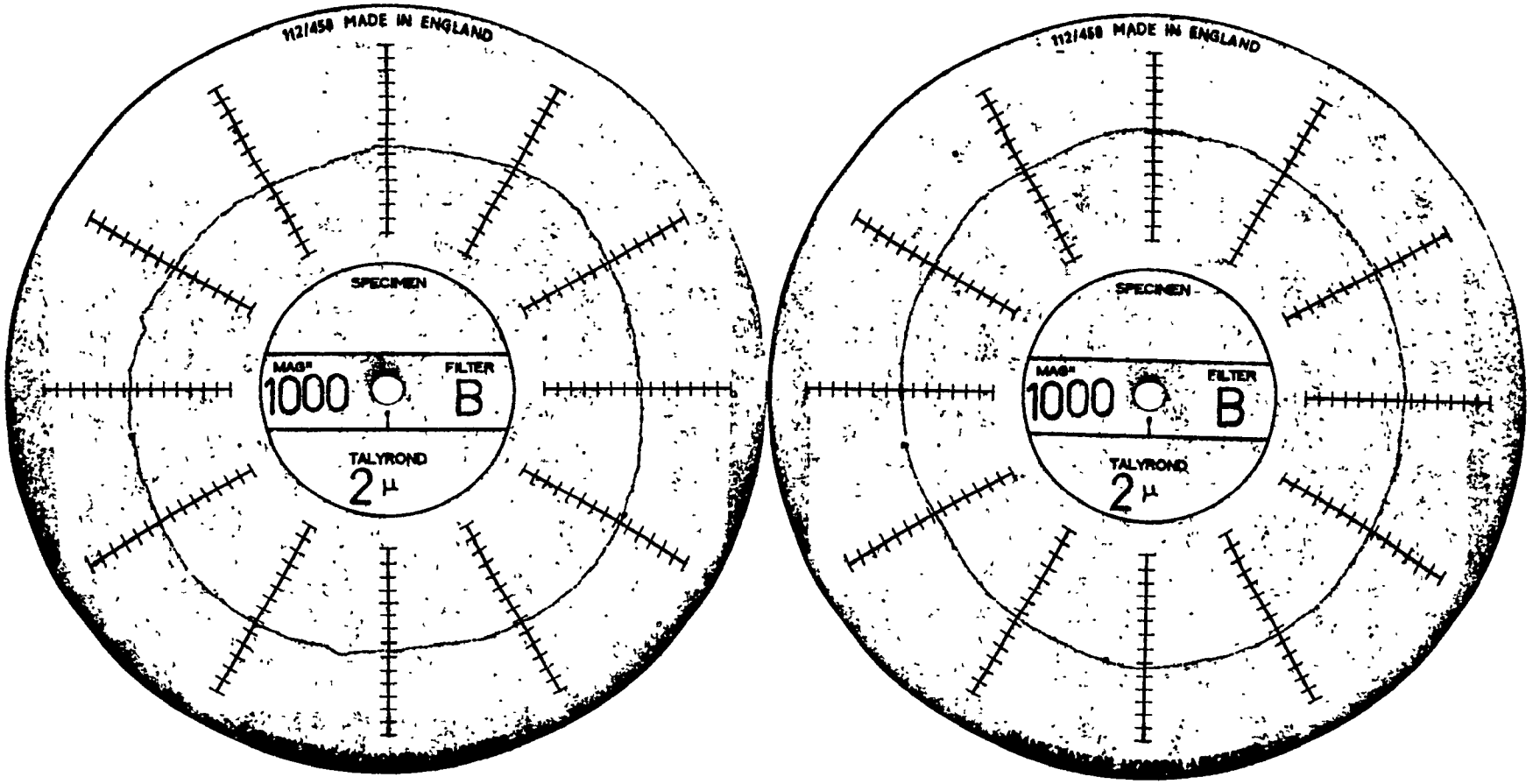

a) b)

Fig. 5.15 Polar plots of holes machined with standard BTA–solid tool and modified BTA–solid tool

CHAPTER 6

SUMMARY AND CONCLUSION

6.1 Conclusion

The major aim of this thesis was to identify spiralling and give possible remedies for it. In some of the cases of spiralling the phenomenon was repeatable for a constant speed and in some instances it was not dependent on the speed. The repeatable spirals were formed for a limited hole depth only, while the random spiralling was present throughout the entire depth of the workpiece.

Since the tool is rigidly connected to the boring bar, any forced input arising from the cutting action occurs at a fixed relative position on the boring bar-tool assembly. Because of this phenomenon, the study of the model of the boring bar-tool assembly was important. Since the workpiece was relatively more rigid, the need to study in depth the model of the workpiece-spindle assembly did not arise.

The first step of the investigation was the identification of the lateral (bending) natural frequencies of the boring bar-tool assembly which was experimentally performed. The next stage in the work was to run the machine at speeds that multiples of the lateral natural frequencies of the boring bar-tool assembly for different workpiece materials. As shown by experimental results in

Chapter 5, spiralling was induced only at five lobes and it occurred repeatedly for different materials at the same operating conditions. It was also shown that spiralling can occur for any speed while using a defective tool having its circle-land slightly oversize.

It was also shown that spiralling can be prevented by modifying the BTA-solid tool. This was done by inserting an additional small pad behind the cutter to prevent its digging deep into the surface of the bore wall or by modifying the BTA-solid tool by giving the circle-land a pad.

The spiralling phenomenon can be prevented by avoiding critical frequencies and ensuring that the tool is in good condition. However since the lateral natural frequencies change over the length of the workpiece a great deal, especially for long workpieces, there is a possibility of one of the fundamental frequencies coinciding with spiral frequency.

The modified BTA-solid tool with a third pad behind the circle-land ensures that spiralling will not occur by preventing it from digging the bore surface. The major advantage of this tool is that one can operate at any speed even at speeds where the natural lateral frequency coincides with the appropriate spiral frequency.

Another way of preventing the spiralling phenomenon is having the circle-land slightly undersize relative to the position of the pads on the circumference of the tool

(50μm). However this was tested only for some materials with low shear strength and there is no guarantee that spiralling will not occur at all. Consequence however would be a serious drawback associated with the bore undersize.

6.2 Application in Industry

The results of this investigation are of great importance for industry dealing with deep-hole boring equipment. Since spiralling accounts for the scraping of highly expensive parts being manufactured, it is crucial that the phenomenon be identified and solved at machine shop floor.

Application of the remedies of prevention of spiralling phenomenon is simple and inexpensive. The third pad introduced behind the cutter was comparatively small in size. Since for most applications the current trend is to use disposable indexable carbide inserts the pad could be manufactured as an integral part of the outer cutter. This will prevent the circle land from digging deep into the surface of the bore and yield a better surface finish. The modified type BTA-solid tool will be easy to manufacture accurately as it can be ground after the cutting edges and pads are brazed on the body.

Tools with disposable indexable insert are bound to have errors in size. Hence, this approach will ensure that spiralling will be prevented even for defective tools having circle land oversize due to prevention of digging in

of circle land.

6.3 Recommendations for Future Work

This investigation mainly concentrated on the BTA-solid boring tool. Apparently the BTA-solid boring tool is not the only tool that yields spiralling. There are a number of BTA tools that may yield spiralling at various lobe numbers. It will be advantageous to investigate those tools by undertaking similar study to identify the mechanism by which spiralling is generated.

This work can be further extended by trying to find an exact correlation between the material properties, bluntness of the tool and spiralling, so that it can be predicted without doubt. However the remedy recommended for solid boring tools, as it has been proven experimentally, will serve as a universal means for spiralling prevention.

The slight drawback associated with a third pad as suggested is that run-out error could occur if the starting bushing is slightly misaligned. This however could be an advantage if the bushing is accurately aligned because run-out will be minimal due to a three point guidance.

6.4 Summary

The major find of this thesis on spiralling can be listed as follows:

1) The phenomenon of spiralling can be identified by the clear marks visible twisting along the length of the

hole, in the form of a helix.

2) The BTA-solid tool yields spiralling only in five lobes for the given geometry of the tool and never gave lobes other than five.

3) The two mechanisms for the formation of spiralling were identified based on experiments on different materials, however the location of the cutters and the pads was the dominant factor in the number of lobes formed.

4) A major factor affecting the formation of spiralling is the relative position of the circle-land on the nominal circumference of the hole i.e. a slight oversize of the circle-land (50μm).

5) Another major factor affecting spiralling is a combination of natural frequency, bluntness of the tool and material with low machinability index. If the lateral natural frequency of the boring bar-tool assembly coincides with the spiralling frequency then chances that spiralling will occur are very high.

Based on the above findings, the only logical solution to this problem was given in the form of a pad behind the cutter which prevents spiralling and also improves the surface finish by preventing the circle-land from digging in deep into the bore wall surface.

The results of this investigation with relatively small size tools are equally applicable to large size tools as well, including for trepanning applications. The

improvement suggested will prevent spiralling and yield a smooth surface finish irrespective of the cutting conditions.

REFERENCES

[1] Latinovic, V.N., "An Investigation of the Theoretical and Design Aspects of Unsymmetrical Multi-Cutting Action in Deep-Hole Machining",D. Eng. Thesis, Concordia Univ., Montreal, 1978.

[2] Steeds, W., "A History of Machine Tools 1700-1910 ", Oxforb at the Clarendon Press,1969

[3] Shaw, M.C., "Metal Cutting Principles", Oxford Press, 1984.

[4] Pepper, H., "Deep Hole Drilling With H. S. S. Twist Drills", Second International Conference on Deep-Hole Boring and Drilling, May,1977.

[5] Calvin, F. H. and Stanley, F. A., "Turning and Boring Practice", McGraw-Hill Book Company, Inc., 1984

[6] Renz, M. and Cawdery, D. O., "The Concept of Gun Drilling, Design and Development of Machines and Tools" First International Conference on Deep-Hole Boring and Drilling, May, 1975.

[7] Panton, R., "The Ejector Drill System" Second International Conference on Deep-Hole Boring and Drilling, May, 1977.

[8] Faber, K., "Deep Hole Drilling Using the Ejector System",First International Conference on Deep-Hole Boring and Drilling, May, 1975.

[9] Swinehart, H. J., "Gundrilling, Trepanning and

Deep-Hole Machining", ASTME, Dearborn, 1976.

[10] Merchant, M. E., "Basic Mechanics of the Metal Cuttting Process", Journal of Applied Mechanics, Volume 11,1944 (pp 168-175).

[11] Merchant, M. E., "Mechanics of the Metal Cutting Process in Orthogonal Cutting and a Type 2 Chip", Journal of Applied Physics, Volume 16, No. 5, 1945 (pp 267-275).

[12] Rakhit, A. K., Sankar, T. S. and Osman, M. O. M., "An Experimental Investigation in the Random Cutting Forces and Surface Roughness Characteristics in a Turning Operation",

[13] Arnold, R. N., "The Mechanics of Tool Vibration in the Cutting of Steel", Proceeding Institute of Mechanical Engineers, Volume 154, 1946.

[14] Tobias, S. A. and Fishwick, W., "The Chatter of Lathe Tools Under Orthogonal Cutting Conditions", Proceedings of ASME, June, 1957.

[15] Merritt, H. E., "Theory of Self-Excited Machine-Tool Chatter, Contribution to Machine Tool Chatter Research-1", Journal of Engineering for Industry, Nov., 1965.

[16] Long, G. W. and Lemon, J. R., "Structural Dynamics in Machine Tool Chatter, Contribution to Machine-tool Chatter, Research-2", Journal of Engineering for Industry, Nov., 1965.

[17] Kegg, R. L., "Cutting Dynamics in Machine Tool

Chatter, Contribution to Machine-Tool Chatter Research-3", Journal of Engineering for Industry, Nov., 1965.

[18] Lemon, J. R. and Ackerman, P. C., "Application of Self-Excited Machine Tool Chatter theory, Contribution to Machine-Tool Chatter, Research-4", Journal of Engineering for Industry, Nov., 1965.

[19] William Wu, D., "Governing Equations of the Shear Angle Oscillation in Dynamic Orthogonal Cutting", Journal of Engineering for Industry, Vol. 108, Nov., 1986.

[20] Fujii, H., Marui, E. and Ema, S., "Whirling Vibrations in Drilling. Part 1: Cause of Vibration and Role of Chisel Edge", Journal of Engineering for Industry, Vol. 108, Aug., 1986.

[21] Fujii, H., Mauri, E. and Ema, S., "Whirling Vibrations in Drilling. Part 2: Influence of Drilling Geometries, Particularly of the Drill Flank, on the Initiation of Vibration", Journal of Engineering for Industry, Vol. 108, Aug., 1986.

[22] Fujii, H., Mauri, E. and Ema, S., "Whirling Vibrations in Drilling. Part 3: Vibration analysis in Drilling Workpiece with a Pilot Hole", Journal of Engineering for Industry, Vol. 110, Nov., 1988.

[23] Ema, S., Fujii, H. and Marui, E., "Chatter Vibration in Drilling", Journal of Engineering for Industry, Vol. 110, Nov., 1988.

[24] Sakuma, K., Taguchi, K. and Katsuki, A, "Study on Deep-Hole Drilling With Solid Boring Tools. The Effect of Tool Materials on the Cutting Performance", Bulletin of the JSME, Vol. 21, No. 153, March, 1978.

[25] Sakuma, K., Taguchi, K. and Katsuki, A, "Study on Deep-Hole Boring by BTA System Solid Boring Tool. Behavior of Tool and its Effects of Profile of Machined Hole", Bulletin of JSPE, Vol. 14, No. 3, Sept., 1980.

[26] Sakuma, K., Taguchi, K. and Katsuki, A, "Study on Deep-Hole Drilling With Solid Boring Tools. The Burnishing Action of Guide Pads and Their Influence on Hole Accuracies", Bulletin of the JSME, Vol. 23, No. 185, Nov., 1980.

[27] Sakuma, K., Taguchi, K., Katsuki, A and Takeyama, H., "Self-Guided Action of Deep-Hole Drilling Tools", Annals CIRP, 30(1), 1981.

[28] Cronjäger, L., Stokert, R. and Weber, U., "Vibrations and Their Effects on Accuracy in Deep-Hole Boring", Third International Conference on Deep-Hole Boring and Drilling, May, 1979.

[29] Griffiths, B. J., "An Introduction to Deep-Hole Drilling and Boring", First International Conference on Deep-Hole Boring and Drilling, May, 1975.

[30] Griffiths, B. J., "Deep-Hole Drilling Process and Surface Integrity", Second International Conference

on Deep-Hole Boring and Drilling, May, 1977.

[31] Griffiths, B. J., "Guidelines for Planning A Deep Hole Drilling ("Self-Piloted Drilling") Operations", Second International Conference on Deep-Hole Boring and Drilling, May, 1977.

[32] Greuner, B. J., "Deep-Hole Boring and Finishing Techniques and Their Applications to the Manufacture of Hydraulic Cylinders", Second International Conference on Deep-Hole Boring and Drilling, May, 1977.

[33] Greuner, B. J., "New Aspects in the Field of Deep-Hole Boring", Second International Conference on Deep-Hole Boring and Drilling, May, 1977.

[34] Greuner, B. J., "Recent Developments and Current Trends in Deep-Hole Boring", Third International Conference on Deep-Hole Boring and Drilling, May, 1979.

[35] Tuffentsammer, K., "Feasibility of Controlled Adaption in Deep-Hole Boring", Second International Conference on Deep-Hole Boring and Drilling, May, 1977.

[36] Latinovic, V. N. and Osman, M. O. M., "On the Performance of Unsymmetrical Multi-Edge Tools for BTA Hole Machining-Test Results", Sixth North American Metal Working Research Conference Proceedings, April 16-19, 1978, (pp 317-323).

[37] Latinovic, V. N. and Osman, M. O. M., "Optimal

Design of BTA Deep-Hole Cutting Tools With Staggerwd Cutters", International Journal of Production Research, Vol. 27, No. 1, 1989.

[38] Torabi, S.J. and Latinovic, V.N., "Improved Version of Optimal BTA Tools with Staggered Disposable Carbide Inserts", CSME Mech. Eng. Forum, Toronto, 1990.

[39] Buck, G., "Chip Forms in Drilling With Gun Drills", First International Conference on Deep-Hole Boring and Drilling, May, 1975.

[40] Streicher, P., "Drilling With Long Gun Drills", Second International Conference on Deep-Hole Boring and Drilling, May, 1977.

[41] Pfleghar, F., "The Aspect of Stability in Designing Deep-Hole Drilling and Boring Tools", Second International Conference on Deep-Hole Boring and Drilling, May, 1977.

[42] Zwingmann, G., "Cooling Lubricants for Deep Drilling", First International Conference on Deep-Hole Boring and Drilling, May, 1977.

[43] Weber, U., "Distribution of Load and Balance of Energy in Deep-Hole Boring", Second International Conference on Deep-Hole Boring and Drilling, May, 1977.

[44] Chandrashekar, S., "An Analytical and Experimental Stochastic Modelling of the Resultant Force System in BTA Deep-Hole Machining and its Influence on the

Dynamics of the Machine Tool Workpiece System", Ph. D. Thesis, Concordia Univ., Montreal, 1984.

[45] Kronenberg, M., "Machining Science and Applications, Theory and Practice for Operation and Development of Machining Processes", Pergamon Press Inc., 1966.

[46] Gessesse, Y. B. and Latinovic, V. N., "Effects of the Stiffness Characteristics of the Stuffing Box on Boring Bar Vibrations", International Journal of Production Research, (accepted Aug. 1990).

[47] Griffiths, B. J., "An Investigation into the Role of the Burnishing Pads in the Deep Hole Drilling Process", Ph. D. Thesis, Brunel University, July 1982.

[48] DeSalvo, G. J. and Gorman, L. W., "ANSYS Engineering Analysis Systems User's Manual", Swanson Analysis Systems Inc., June 1, 1987.

APPENDIX A

THE FINITE ELEMENT MODEL AND MODAL ANALYSIS

This appendix gives the derivation of the finite element method and modal analysis based on the finite element method approach.

Taking into consideration a single element whose end conditions are given as shown in Fig. A1 the deflection of the element at any distance x from 0 and at any time t is given by eqn. A.1, this equation was derived using the assumed modes method.

$$u(x,t) = \sum_{i=1}^{4} \psi_i(x)\, u_i(t) \qquad (A.1)$$

where the function $\psi_i(x)$ satisfies the boundary conditions given by:

$$\begin{aligned}
&\psi_1(0) = 1, \quad \psi_1'(0) = \psi_1(L_{st}) = \psi_1'(L_{st}) = 0 \\
&\psi_2'(0) = 1, \quad \psi_2(0) = \psi_2(L_{st}) = \psi_2'(L_{st}) = 0 \\
&\psi_3(L_{st}) = 1, \quad \psi_3(0) = \psi_3'(0) = \psi_3'(L_{st}) = 0 \\
&\psi_4'(0) = 1, \quad \psi_4(0) = \psi_4'(L_{st}) = \psi_4(L_{st}) = 0
\end{aligned} \qquad (A.2)$$

a) Beam loading

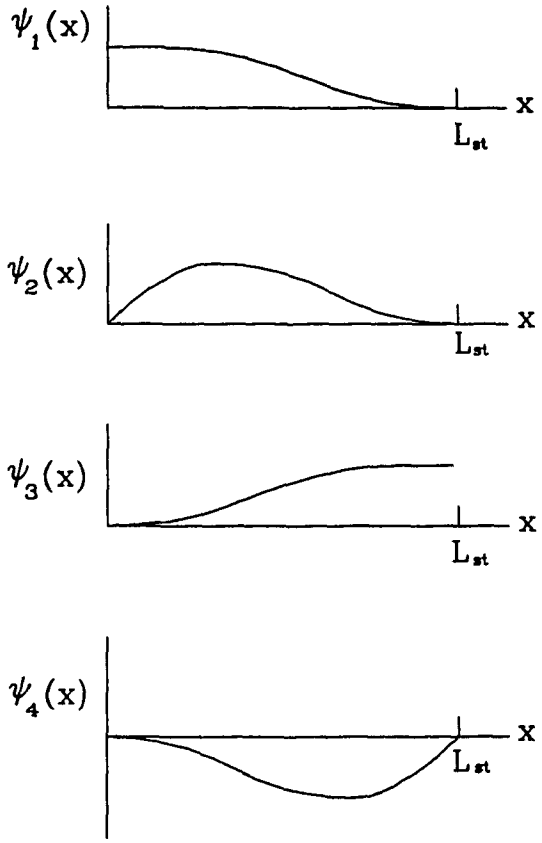

b) Shape function

Fig. A.1 Shape functions for transverse deformation of a beam

Assuming that the finite element is loaded in shear only the equation of equilibrium is given as:

$$(E_{st} I_{st} u'')'' = 0 \qquad \text{(A.3)}$$

The general solution of equation A.3 is given as:

$$u(x) = C_1 + C_2\left(\frac{x}{L_{st}}\right) + C_3\left(\frac{x}{L_{st}}\right)^2 + C_4\left(\frac{x}{L_{st}}\right)^3 \qquad \text{(A.4)}$$

where x/L_{st} was used to keep the dimensions of the constants the same. Substituting the four sets of boundary conditions of eqn. A.2 into eqn. A.4, the shape functions given by equation A.5 are obtained.

$$\psi_1 = 1 - 3\left(\frac{x}{L_{st}}\right)^2 + \left(\frac{x}{L_{st}}\right)^3$$

$$\psi_2 = x - 2L_{st}\left(\frac{x}{L_{st}}\right)^2 + \left(\frac{x}{L_{st}}\right)^3 \qquad \text{(A.5)}$$

$$\psi_3 = 3\left(\frac{x}{L_{st}}\right)^2 + 2\left(\frac{x}{L_{st}}\right)^3$$

$$\psi_4 = -L_{st}\left(\frac{x}{L_{st}}\right)^2 + L_{st}\left(\frac{x}{L_{st}}\right)^3$$

The kinetic energy and the potential energy of the element are derived from the specified displacement

functions properties of the element such as the cross sectional area, density, elasticity and moment of inertia. Therefore the kinetic energy is:

$$T = \frac{1}{2} \int \rho A_{st} (\psi_i \dot{u}_i)^2 dx$$

$$= \frac{1}{2} \sum_{i=1}^{4} \sum_{i=1}^{4} M_{ij} \dot{u}_i \dot{u}_j \qquad (A.6)$$

$$\text{where } M_{ij} = \int_0^1 \rho A_{st} \psi_i \psi_j dx \qquad (A.7)$$

Similarly the potential energy expression is derived from the elements stiffness properties and given as:

$$V = \frac{1}{2} \int_0^1 E_{st} I_{st} (\psi_i'' \psi_j'')^2 dx$$

$$= \frac{1}{2} K_{ij} u_i u_j \qquad (A.8)$$

$$\text{where } K_{ij} = \int_0^1 E_{st} I_{st} \psi_i'' \psi_j'' dx \qquad (A.9)$$

Finally the Lagrange's equation will be used to write the equation of motion of the element.

$$\frac{d}{dt} \left(\frac{\partial T}{\partial \dot{q}_i} \right) - \frac{\partial T}{\partial q_i} + \frac{\partial V}{\partial q_i} = Q_i \qquad (A.10)$$

Using the Lagrange's equation on the element the mass matrix and stiffness matrix can be calculated to give equations (A.11) and (A.12) respectively.

$$[M] = \frac{\rho A_{st} L_{st}}{420}\begin{bmatrix} 156 & 22L_{st} & 54 & -13L_{st} \\ & 4L_{st}^2 & 13L_{st} & -3L_{st}^2 \\ & & 156 & -22L_{st} \\ \text{SYM} & & & 4L_{st}^2 \end{bmatrix} \qquad \text{(A.11)}$$

$$[K] = \frac{E_{st} I_{st}}{L_{st}^3}\begin{bmatrix} 12 & 6L_{st} & -12 & 6L_{st} \\ & 4L_{st}^2 & -6L_{st} & 2L_{st}^2 \\ & & 12 & -6L_{st} \\ \text{SYM} & & & 4L_{st}^2 \end{bmatrix} \qquad \text{(A.12)}$$

Applying the direct stiffness method which implies that, since the work and energy of a structure are scalar quantities, the total strain energy of the beam or structure is the sum of the strain energy contributions of all of its elements, the individual matrices of the elements can be assembled.

For this particular example the assembly brings together two adjacent matrices by adding the elements (3,3), (3,4), (4,3) and (4,4) of the first matrix to (1,1), (1,2), (2,1) and (2,2) of the second matrix respectively. Similarly elements (3) and (4) of the first force vector are added with elements (1) and (2) of the second force vector. Performing this assembly sequentially results in the finite element equation consisting of the mass matrix and stiffness matrix.

Solving the above linear sets of equations gives a number of eigen values and eigen vectors. The eigen vectors also known as the natural modes are assembled in columns to form the modal matrix. Using this matrix to transform the equations to the principal coordinate system q_i by premultiplying with its transform and post multiplying with the original matrix, the mass and stiffness matrices, provides a set of decoupled equations.

The above decoupled equations can be easily solved and transformed to the original coordinate system to give the mode shapes in world coordinate.